



HAL
open science

Regioselective and Stereoselective Synthesis of Parthenolide Analogs by Acyl Nitroso-Ene Reaction and Their Biological Evaluation against *Mycobacterium tuberculosis*

Bruna Gioia, Francesca Ruggieri, Alexandre Biela, Valérie Landry, Pascal Roussel, Florence Leroux, Ruben C Hartkoorn, Nicolas Willand

► To cite this version:

Bruna Gioia, Francesca Ruggieri, Alexandre Biela, Valérie Landry, Pascal Roussel, et al.. Regioselective and Stereoselective Synthesis of Parthenolide Analogs by Acyl Nitroso-Ene Reaction and Their Biological Evaluation against *Mycobacterium tuberculosis*. *International Journal of Molecular Sciences*, 2023, 24 (24), pp.17395. 10.3390/ijms242417395 . hal-04339224

HAL Id: hal-04339224

<https://hal.science/hal-04339224>

Submitted on 12 Dec 2023

HAL is a multi-disciplinary open access archive for the deposit and dissemination of scientific research documents, whether they are published or not. The documents may come from teaching and research institutions in France or abroad, or from public or private research centers.

L'archive ouverte pluridisciplinaire **HAL**, est destinée au dépôt et à la diffusion de documents scientifiques de niveau recherche, publiés ou non, émanant des établissements d'enseignement et de recherche français ou étrangers, des laboratoires publics ou privés.



Distributed under a Creative Commons Attribution 4.0 International License



Article

Regioselective and Stereoselective Synthesis of Parthenolide Analogs by Acyl Nitroso-Ene Reaction and Their Biological Evaluation against *Mycobacterium tuberculosis*

Bruna Gioia ¹, Francesca Ruggieri ¹, Alexandre Biela ¹, Valérie Landry ¹, Pascal Roussel ², Catherine Piveteau ¹, Florence Leroux ¹, Ruben C. Hartkoorn ³ and Nicolas Willand ^{1,*}

¹ Univ. Lille, Inserm, Institut Pasteur de Lille, U1177—Drugs and Molecules for living Systems, F-59000 Lille, France; bruna.gioia@univ-lille.fr (B.G.); francesca.ruggieri@univ-lille.fr (F.R.); alexandre.biela@pasteur-lille.fr (A.B.); valerie.landry@pasteur-lille.fr (V.L.); catherine.piveteau@univ-lille.fr (C.P.); florence.leroux@pasteur-lille.fr (F.L.)

² Univ. Lille, CNRS, ENSCL, Centrale Lille, Univ. Artois, UMR 8181—UCCS—Unité de Catalyse et de Chimie du Solide, F-59000 Lille, France; pascal.roussel@univ-lille.fr

³ Univ. Lille, CNRS, Inserm, CHU Lille, Institut Pasteur de Lille, U1019—UMR 8204—CIIL—Center for Infection and Immunity of Lille, F-59000 Lille, France; ruben.hartkoorn@inserm.fr

* Correspondence: nicolas.willand@univ-lille.fr

Abstract: Historically, natural products have played a major role in the development of antibiotics. Their complex chemical structures and high polarity give them advantages in the drug discovery process. In the broad range of natural products, sesquiterpene lactones are interesting compounds because of their diverse biological activities, their high-polarity, and sp³-carbon-rich chemical structures. Parthenolide (PTL) is a natural compound isolated from *Tanacetum parthenium*, of the family of germacranolide-type sesquiterpene lactones. In recent years, parthenolide has been studied for its anti-inflammatory, antimigraine, and anticancer properties. Recently, PTL has shown antibacterial activities, especially against Gram-positive bacteria. However, few studies are available on the potential antitubercular activities of parthenolide and its analogs. It has been demonstrated that parthenolide's biological effects are linked to the reactivity of α -exo-methylene- γ -butyrolactone, which reacts with cysteine in targeted proteins via a Michael addition. In this work, we describe the ene reaction of acylnitroso intermediates with parthenolide leading to the regioselective and stereoselective synthesis of new derivatives and their biological evaluation. The addition of hydroxycarbamates and hydroxyureas led to original analogs with higher polarity and solubility than parthenolide. Through this synthetic route, the Michael acceptor motif was preserved and is thus believed to be involved in the selective activity against *Mycobacterium tuberculosis*.

Keywords: natural products; semisynthesis; *Mycobacterium tuberculosis*



Citation: Gioia, B.; Ruggieri, F.; Biela, A.; Landry, V.; Roussel, P.; Piveteau, C.; Leroux, F.; Hartkoorn, R.C.; Willand, N. Regioselective and Stereoselective Synthesis of Parthenolide Analogs by Acyl Nitroso-Ene Reaction and Their Biological Evaluation against *Mycobacterium tuberculosis*. *Int. J. Mol. Sci.* **2023**, *24*, 17395. <https://doi.org/10.3390/ijms242417395>

Academic Editor: Jose Javier Sanz-Gómez

Received: 3 November 2023

Revised: 30 November 2023

Accepted: 8 December 2023

Published: 12 December 2023



Copyright: © 2023 by the authors. Licensee MDPI, Basel, Switzerland. This article is an open access article distributed under the terms and conditions of the Creative Commons Attribution (CC BY) license (<https://creativecommons.org/licenses/by/4.0/>).

1. Introduction

Natural products (NPs) and their derivatives have always been an important source of new medicines. Natural products often have complex chemical structures and can exhibit a wide range of biological activities, making them valuable starting points in the drug discovery process. Compared with conventional synthetic molecules, NPs are sometimes also more polar, which is an advantage in the discovery of new targets [1]. In the vast range of NPs, sesquiterpene lactones are compounds of interest for their structural complexity and diversity. Parthenolide (PTL) is a germacranolide-type sesquiterpene lactone isolated from *Tanacetum parthenium* [2]. For decades, PTL has been known for its anti-inflammatory and antimigraine effects [3]. The wide range of biological activities shown by PTL is mainly attributed to the α -exo-methylene- γ -butyrolactone moiety present in its structure [4,5]. In fact, α -exo-methylene is able to react with nucleophilic cysteines from biomolecules through a Michael addition (Figure 1) [6–8] to form a covalent bond.

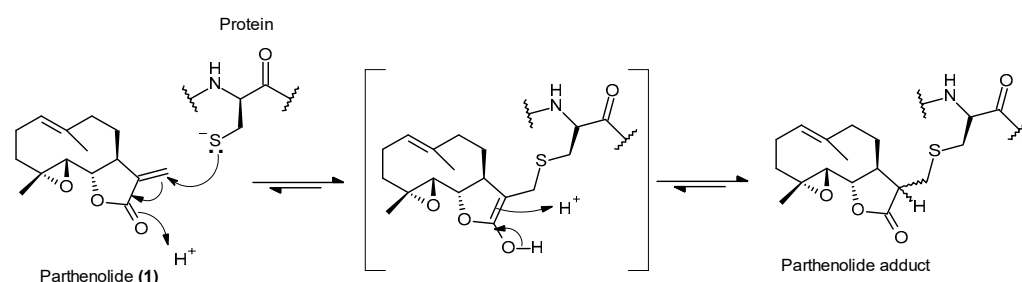


Figure 1. Biological reactivity of parthenolide in the presence of a cysteine residue in a protein attacking the β -carbon of the Michael acceptor.

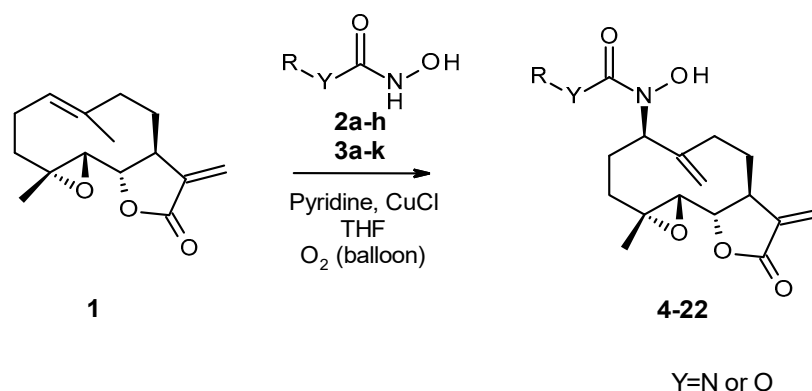
Through this mechanism, PTL inhibits irreversibly the NF- κ B pathway, which is involved in anti-inflammatory activity, in the regulation of cell proliferation, and in anti-apoptotic mechanisms [9]. Parthenolide reacts with thiols from glutathione, leading to the depletion of GSH and consequent activation of the ROS cascade [10,11]. Precisely for all these targets, parthenolide is well-known as an anticancer agent. Many studies have been carried out through the chemical modification of PTL, mainly focusing on α -*exo*-methylene, including (i) a Michael addition with primary and secondary amines and thiol groups with increasing solubility [12–15] and (ii) Heck coupling with aromatic iodo-compounds [16]. All these studies have shown important advances in the anticancer properties of parthenolide [11,17]. More recently, interest in PTL as an antibacterial agent has grown. Hakkinen et al. studied the activity against Gram-positive and Gram-negative bacteria, and PTL showed higher activity against *Staphylococcus aureus* (*S. aureus*) than against Gram-negative bacteria, such as *Pseudomonas aeruginosa* and *Escherichia coli* [18,19]. Few studies have investigated the activity against *Mycobacterium tuberculosis* (*M. tuberculosis*) [20–22]. PTL displayed a minimum inhibitory concentration (MIC) of 16 μ g/mL against *M. tuberculosis* strains, but no further investigation has been carried out on the structure–activity relationship or target identification [22]. Hence, we planned the synthesis of original parthenolide-based derivatives using an acylnitroso-ene reaction, which were evaluated as antibacterial agents and, more precisely, as anti-tuberculosis drugs. With this work, we optimize a regioselective and stereoselective synthetic route for original analogs. Through an acyl nitroso-ene modification, the Michael acceptor motif is preserved. Moreover, owing to the introduction of the hydroxylamine moiety on the main core, the new semisynthetic analogs displayed increased solubility compared to that of the parent compound.

2. Results and Discussion

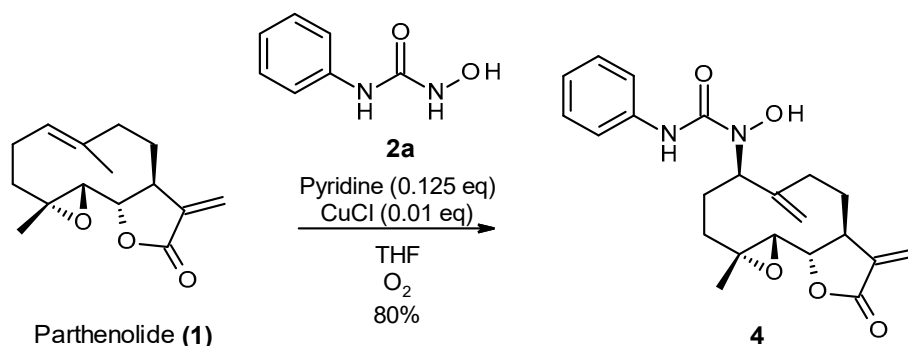
2.1. Chemistry

C-7-hydroxycarbamate/urea–parthenolide analogs were synthesized from commercially available parthenolide via a reaction with hydroxylamine-functionalized building blocks (Scheme 1). First, the optimization was performed, starting from the conditions previously described by Frazier et al. [23]. The critical step in the acylnitroso-ene reaction is the oxidation of hydroxylamine-containing compounds to nitroso derivatives prior to the reaction with parthenolide.

Therefore, an optimization step was necessary to identify the best conditions and the best oxidative system. Different reaction times, equivalents, and oxidant agents were investigated in a model reaction with 1-hydroxy-3-phenyl-urea (2a). All the studied conditions are available in the supplementary information. After the optimization, oxygen was chosen as oxidizing agent, and the reaction was carried out in the presence of a catalyst system of CuCl (0.05 eq.), pyridine (0.125 eq.), and THF as the solvent (Scheme 2).



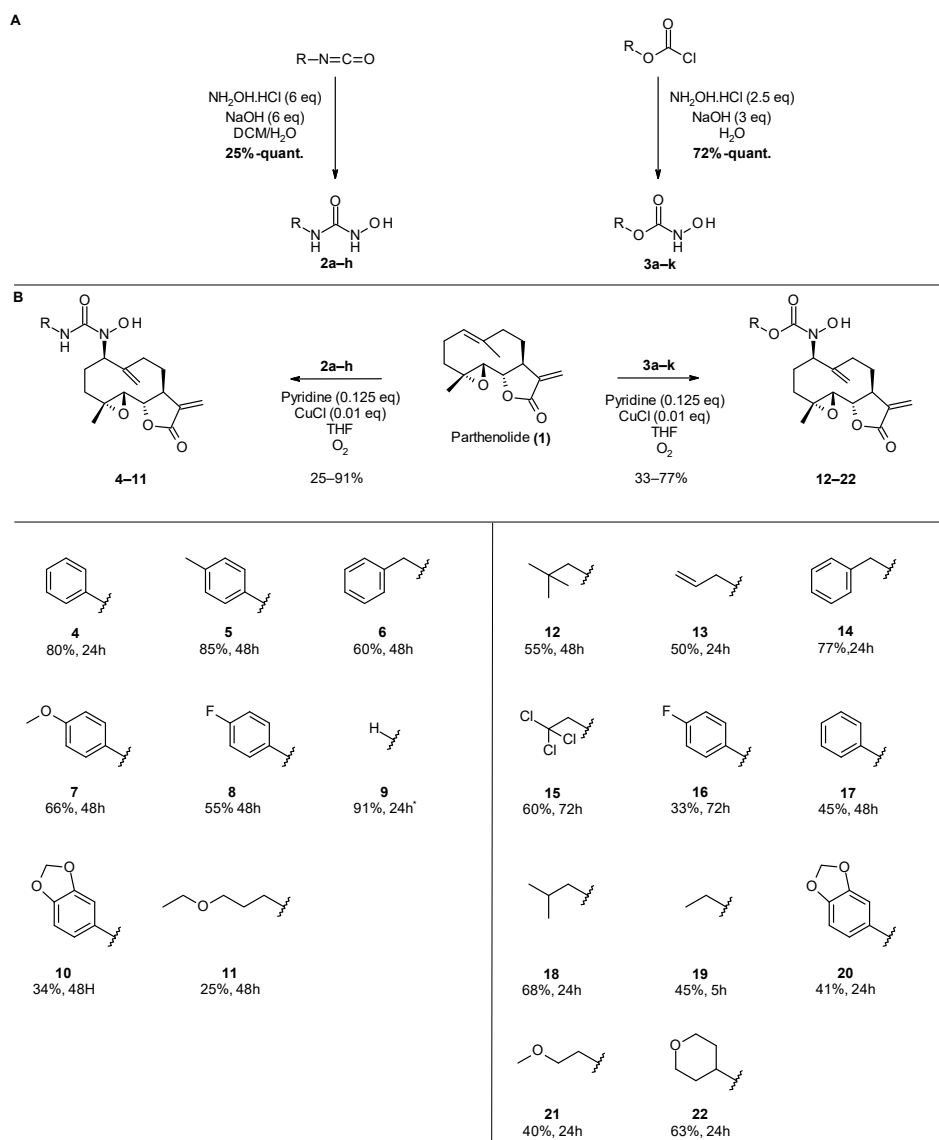
Scheme 1. Overview of the acylnitroso-ene reaction between parthenolide and hydroxyureas (Y = NH) or hydroxycarbamates (Y = O).



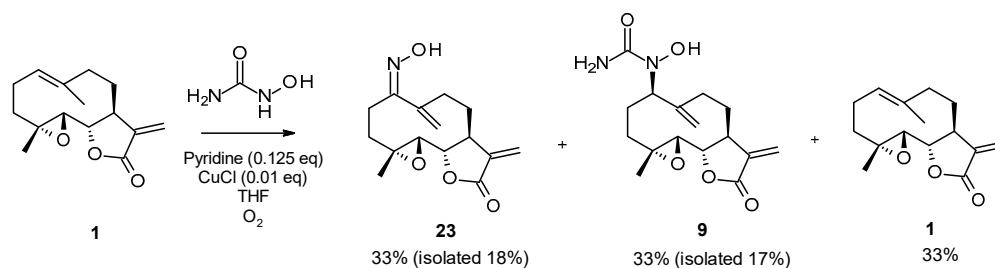
Scheme 2. Optimized conditions of acylnitroso-ene reaction between parthenolide and 1-hydroxy-3-phenyl-urea.

To expand the scope of this reaction, two series of compounds were synthesized based on hydroxylamine-containing functions: hydroxyurea and hydroxycarbamate, either purchased or synthesized. Urea (2a–h) and carbamate (3a–k) precursors were obtained from isocyanates and chloroformates, respectively (Scheme 3A). Unfortunately, the introduction of more hydrophilic moieties was challenging owing to the high polarity of the corresponding ureas. In fact, after the work-up, urea precursors were isolated as a mixture of the expected compound, salts, and HCl residues, which prevented the formation of nitroso-ene compounds. On the other hand, ureas bearing aromatic substituents were easily accessed. Hydroxycarbamates with polar and less-polar groups were easily obtained in good to high yields. Parthenolide reacted with a variety of substrates, from some polar alkyl groups to more lipophilic aromatic substituents (Scheme 3B) under the optimized conditions in Scheme 2. As a result, nineteen original compounds were obtained in yields ranging from 25 to 91%.

Moreover, it must be noted that the reaction between the parthenolide and hydroxyurea led to the formation of two compounds (Scheme 4). In fact, it was observed that after 48 h, a mixture of the parthenolide, hydroxyurea derivative (9), and side compound corresponding to the oxime derivative (23) was obtained. Compound 23 was then isolated, and a biological assessment was carried out. Surprisingly, the removal of the O₂ supply resulted in the formation of hydroxyurea (9) in a very good yield, and just traces of oxime were observed.



Scheme 3. (A) General synthesis of hydroxycarbamates (**3a–k**) and hydroxyureas (**2a–h**) from isocyanates and chloroformates, respectively. (B) Synthesis of C-7 parthenolide derivatives: hydroxyureas (**4–11**) and hydroxycarbamates (**12–22**). * Compound **9** was obtained by exposure to air without an O₂ supply.

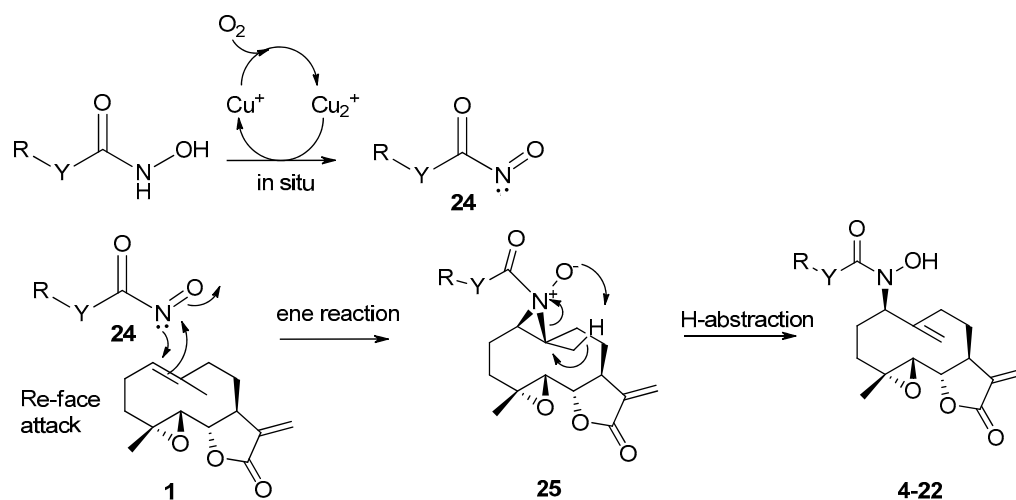


Scheme 4. Nitroso-ene reaction between parthenolide and hydroxyurea. Two compounds were obtained in the presence of O₂: the oxime derivative (**23**) and hydroxyurea derivative (**9**). Moreover, the conversion was not total. Compounds **23** and **9** were isolated after purification under reverse-phase conditions (C-18 column).

Conditions under air were tested for this reaction, and it was observed that O₂ enhanced the acylnitroso-ene reaction, and no formation of oxidized compounds was observed (entry E, Table S1 in Supplementary Materials). To the best of our knowledge, this is the first report of a nitroso-ene reaction with parthenolide under mild conditions and with high stereoselectivity and regioselectivity to give twenty semisynthetic analogs in moderate to good yields.

2.1.1. Proposed Reaction Mechanism

Numerous hypotheses have been postulated for the mechanism of the nitroso-ene reaction, but it has not been totally elucidated yet [24–28]. The ene reaction of nitrosocarbonyl derivatives follows Markovnikov's rule with the addition of the electron-deficient enophile (**24**) to the less-substituted carbon of the alkene (**1**). According to previous studies, we hereby suggest that the reaction takes place through an intermediary aziridinium state (**25**, Scheme 5), which can explain the regioselectivity and stereoselectivity. In an oxidant environment, O₂ leads to oxidation from Cu (I) to Cu (II), then Cu (II) oxidizes the hydroxylamine derivative (**24**, hydroxyurea or hydroxycarbamate) to nitrosocarbonyl species. The combination of CuCl, pyridine, and THF promotes the generation of the transient state of nitroso species in situ [29]. Afterward, a concerted mechanism takes place: the electrophilic nitrogen of **24** attacks the ene species, parthenolide, and, vice versa, the ene attacks the enophile (**24**) leading to the aziridinium intermediate (**25**). The intermediate (**25**), which is unstable, evolves to the final compound by H-abstraction from the more-substituted and less-crowded end, leading to high regioselectivity. The less-hindered *Re*-face attack from the nitroso species is favored, thus conferring high stereoselectivity.



Scheme 5. Proposed mechanism of reaction to explain regioselectivity and stereoselectivity.

2.1.2. X-ray Crystallographic and NOESY Data

In support of our hypothesis, the configuration of the new chiral carbon (C-7) was determined by a NOESY experiment with compound **14**. MOE modelling enabled the determination of four possible structures: two for each configuration *R* or *S* (images are available in Supplementary Materials). For the *R* configuration, both models showed a possible spatial interaction between proton 3 and proton 7 (depicted in green, Figure 2A). On the contrary, for the *S* configuration, the two models showed that proton 7 is in spatial proximity to methyl group 15 (depicted in red, Figure 2B). NOESY spectra determined correlations between H3/H7 and H2/H15, suggesting the *R* configuration for carbon 7. In addition, obtaining the crystallographic structure of **14** enabled us to confirm the exact configuration (Figure 2C).

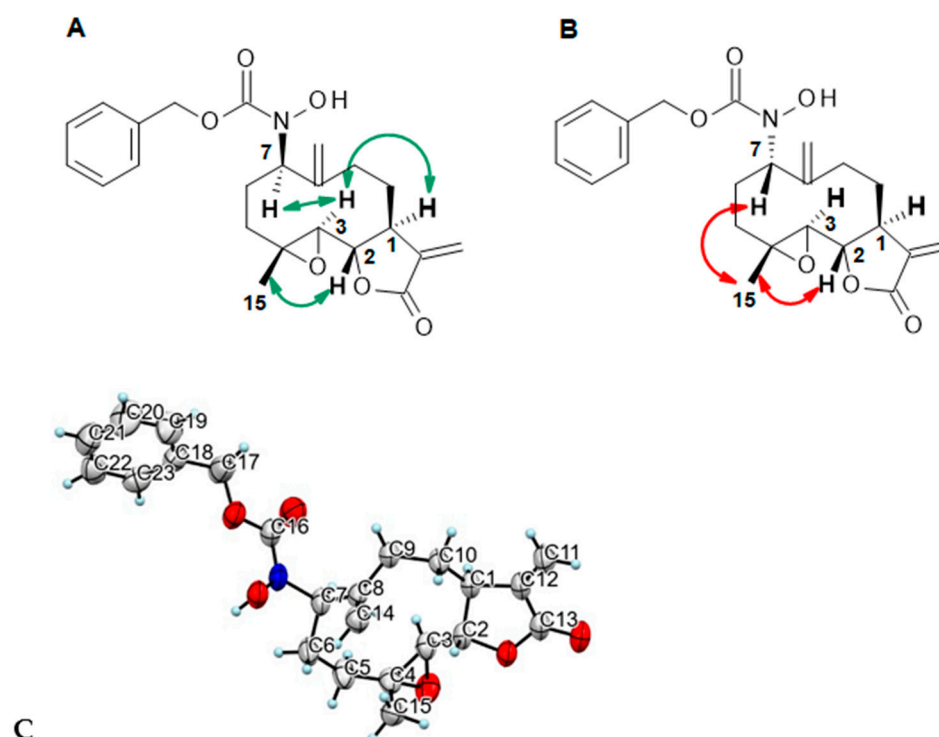
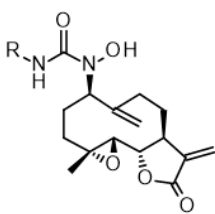
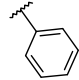
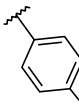
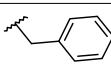
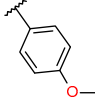
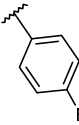
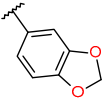
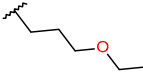


Figure 2. NOESY correlations of compound 14. Possible correlations were identified, using MOE (images in Supplementary Materials), between proton 3 and proton 7 (in green, **A**) corresponding to *R* configuration and between proton 7 and methyl group 15 (in red, **B**) corresponding to *S* configuration. (**C**) ORTEP drawing of compound 14.

2.2. Biological Evaluation

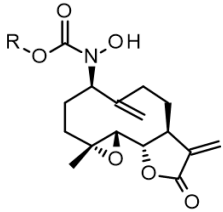


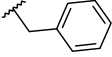
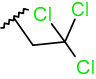
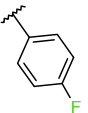
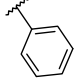
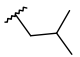

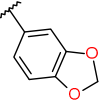
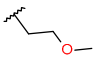
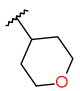
All the synthesized compounds together with parthenolide were tested against the virulent strain *M. tuberculosis* H37Rv and *S. aureus* (Tables 1 and 2). A resazurin microtiter assay (REMA) and a GFP fluorescent assay were performed for *M. tuberculosis*, and a REMA assay was performed for *S. aureus*. The compounds were dissolved in DMSO and tested at eight different concentrations (from 300 μM to 2.3 μM). After a period of incubation (7 days for *M. tuberculosis* and 5 h for *S. aureus*), resazurin was added, and the fluorescence was measured. Rifampicin and DMSO were used as positive and negative controls, respectively. The results were expressed as MIC_{90} (REMA assay) or MIC_{98} (GFP assay) values, meaning that the drug concentration inhibits 90% or 98% of the bacterial growth. All the nitroso-ene derivatives showed antibacterial activity against *M. tuberculosis*. Instead, no activity (MIC_{90} ca. 300 μM) was observed against *S. aureus*. It was observed that bulky groups enhance the activity against *M. tuberculosis*. In fact, compounds 9 and 23 with a hydroxyurea and an oxime moiety, respectively, were found to be inactive (MIC_{90} ca. 150 μM). In accordance with this observation, aromatic substituents were well-tolerated for both series. However, the urea derivatives showed greater inhibitory activity against *M. tuberculosis* strains. The introduction of small substituents, such as a methoxy group (compound 7, Table 1) and a fluorine atom (compound 8, Table 1), to the para position of the benzene ring enhances the inhibitory activity with a MIC_{90} value of 19 μM (REMA assay). Compared with the parent compound, the most active compounds are in the same range of activity (MIC_{90} is between 9.4 μM and 19 μM). However, advantageously, all the nitroso-ene derivatives are more polar and more water soluble than PTL. The urea derivatives (compounds 8 and 9) showed from 1.3- to 1.5-fold higher solubility in PBS compared to parthenolide, respectively.

Table 1. Summary of antibacterial activities against *M. tuberculosis* and *S. aureus*, solubilities, and cytotoxicities of synthesized hydroxyureas (ND is the abbreviation for “not determined”).


Molecule Number	R	MIC ₉₀ <i>M. tuberculosis</i> (μM, REMA)	MIC ₉₈ <i>M. tuberculosis</i> (μM, GFP)	MIC ₉₀ <i>S. aureus</i> (μM, REMA)	Cytotoxicity Balb3T3 CC ₅₀ (μM)	Solubility (μM)
	Rifampicin	<2.3	<2.3	<2.3	ND	ND
1	Parthenolide	9.4–19	9.4–19	>300	>100	135
4		19–38	9.4–19	>300	25	186
5		19–38	19	>300	12.5	186
6		38–75	19–38	>300	>25	196
7		19	19	ND	25	184
8		19	19	ND	>25	188
9	H-	150	75–150	ND	>100	>200
10		38	19	ND	12.5	182
11		150	150	ND	>100	197

As described in the introduction (Section 1), parthenolide reacts with biological nucleophiles through a Michael addition, and it results in potent anticancer agents. Given their unspecific electrophilicity, all the synthesized compounds were also tested for their cytotoxicity activities in Balb3T3 cell lines. The aromatic derivatives showed increased cytotoxicities compared with that of the parent compound. However, the specific activity against *M. tuberculosis* does not seem to be related to cytotoxicity, given the absence of activity against *S. aureus*. At this stage of the investigation, we can only suggest that the Michael acceptor is involved in the activity. In line with our hypothesis, no activity against either *M. tuberculosis* or *S. aureus* was found for Dihydro-PTL (26, Table 2). Extensive studies are needed to discover a possible target and/or perhaps a mechanism of action.

Table 2. Summary of antibacterial activities against *M. tuberculosis* and *S. aureus*, solubilities, and cytotoxicities of synthesized hydroxycarbamates (ND is the abbreviation for “not determined”).

Molecule Number	R	MIC ₉₀		MIC ₉₀ <i>S. aureus</i> (μM, REMA)	Cytotoxicity Balb3T3 CC ₅₀ (μM)	Solubility (μM)
		<i>M. tuberculosis</i> (μM, REMA)	<i>M. tuberculosis</i> (μM, GFP)			
						
	Rifampicin	<2.3	<2.3	<2.3	ND	ND
1	Parthenolide	9.4–19	9.4–19	>300	>100	135
12		38	19–38	>300	>100	176
13		38–75	38	>300	>12.5	192
14		75	38	>300	>12.5	191
15		38	19	>300	12.5	184
16		75	38–75	>300	25	182
17		38	38	ND	12.5	189
18		38	19	ND	50	190
19		75	75	ND	>12.5	198
20		75	37.5–75	ND	>12.5	182
21		150	150–300	ND	100	>200
22		75	38	ND	>50	193
23	Oxime	38–75	38–19	>300	ND	186
26	Dihydro-PTL	300	300	ND	ND	ND

3. Materials and Methods

3.1. Chemistry

The reagents and solvents for synthesis, analysis, and purification were purchased from commercial suppliers (Fisher Scientific (France), Sigma Aldrich (France), Key Organics (UK), and Fluorochem (UK and Ireland)) and used without further purification. The progress of all the reactions was routinely monitored by thin-layer chromatography (TLC) and/or by high-performance liquid chromatography–mass spectrometry (HPLC–MS). TLC was performed using Merck® commercial aluminum sheets coated with silica gel 60 F254. Visualization was achieved by fluorescence quenching under UV light at 254 nm and 215 nm or by staining with potassium permanganate. Purifications were performed by flash chromatography and reverse chromatography. Flash chromatography purifications were conducted in columns prepacked with Reveleris® flash cartridges, Buchi, France (40 µm, Büchi® FlashPure, Villebon sur Yvette, France or 15–40 µm, Macherey-Nagel® Chromabond®, Hoerdt, France) under pressure with an Interchim Puriflash® 430 instrument (Montluçon, France). The products were detected by UV absorption at 254 nm and by ELSD. Reverse chromatographies were conducted using Combiflash® C18 Rf200 in 4g, 12g, and C18 columns (Serlabo Technologies, EntraiguessurlaSorgues, France). The products were detected by UV absorption at 215 nm and 254 nm. UPLC–MS analysis was performed on an LC–MS Waters ACQUITY UPLC I-Class system (Guyancourt, France) equipped with a UPLC I BIN SOL MGR solvent manager, a UPLC I SMP MGR-FTN sample manager, an ACQUITY UPLC I-Class eλ PDA photodiode array detector (210–400 nm), and an ACQUITY QDa (Performance) mass detector (full scan ESI+/- in the range 30–1250). A Waters Acquity BEH C18 column (1.7 µm particle size; dimensions: 50 mm × 2.1 mm) was used for UPLC analysis (Guyancourt, France). The injection volume was 0.5 µL. For a 5 min analysis, the elution was carried out with a gradient starting at 98% H₂O and 5 mM ammonium formate (pH 3.8) and reaching 98% CH₃CN and 5 mM ammonium formate (pH 3.8; 5% aqueous) over 3.5 min at a flow rate of 600 µL/min. For a 30 min analysis, the elution was carried out with a gradient starting at 98% H₂O and 5 mM ammonium formate (pH 3.8) and reaching 98% CH₃CN and 5 mM ammonium formate (pH 3.8; 5% aqueous) over 25 min at a flow rate of 600 µL/min. Purity (%) was determined by reverse-phase UPLC, using UV detection (at 215 and 254 nm). HRMS analyses were performed on an LCT Premier XE Micromass (Guyancourt, France), using a Waters XBridge BEH C18 column with a 3.5 µm particle size and dimensions of 50 mm × 4.6 mm. A gradient starting from 98% H₂O and 5 mM ammonium formate (pH 3.8) and reaching 100% CH₃CN and 5 mM ammonium formate (pH 3.8; 5% aqueous) within 3 min at a flow rate of 2 mL/min was used. NMR spectra were recorded on a Bruker® Avance-300 spectrometer (Wissembourg, France). The results were calibrated to signals from the solvent as an internal reference (e.g., 7.26 (residual CDCl₃) and 77.16 (CDCl₃) ppm and 2.50 (residual DMSO d₆) and 39.52 (DMSO d₆) ppm for ¹H and ¹³C NMR spectra, respectively.) Chemical shifts (δ) are in parts per million (ppm) downfield from tetramethylsilane (TMS). The assignments were made using one-dimensional (1D) ¹H and ¹³C spectra and two-dimensional (2D) HSQC-DEPT, COSY, and HMBC spectra. NMR coupling constants (J) are reported in hertz (Hz), and splitting patterns are indicated as follows: s (singlet); brs (broad singlet); d (doublet); dd (doublet of doublet); ddd (doublet of doublet of doublet); dt (doublet of triplet); t (triplet); td (triplet of doublet); q (quartet); m (multiplet).

3.1.1. General Procedure for the Synthesis of Hydroxyurea Derivatives (2a–h)

In a round-bottom flask, 1.0 eq. of isocyanate was diluted in DCM. Then, 6.0 eq. of hydroxylamine hydrochloride and 6.0 eq. of sodium hydroxide in water were added at 0 °C, and the solution was stirred for 3 h at room temperature. The aqueous layer was extracted once with DCM. The dichloromethane phase was discarded. Then, the aqueous phase was acidified with HCl (1 M) and extracted three times with ethyl acetate. The organic layer was dried over MgSO₄ and concentrated under reduced pressure to give a crude residue. Purification by flash chromatography afforded the desired compound.

1-hydroxy-3-phenyl-urea (**2a**) was obtained as a white powder, without further purification (190 mg, quant.). ^1H NMR (300 MHz, DMSO- d_6) δ = 8.93 (s, 1H); 8.80 (s, 1H); 8.73 (s, 1H); 7.59 (dd, J = 1.11, 8.69 Hz, 2H); 7.23 (t, J = 7.28 Hz, 2H); 6.95 (t, J = 7.28 Hz, 1H). NMR data are in agreement with previously published data [26].

1-hydroxy-3-(*p*-tolyl)urea (**2b**) was obtained as a white powder after purification by flash chromatography in column 15g, with a gradient from 100% dichloromethane to 70/30 dichloromethane/ethyl acetate (257 mg, 41%). ^1H NMR (300 MHz, DMSO- d_6) δ = 8.89 (s, 1H); 8.73 (s, 1H); 8.63 (s, 1H); 7.47 (m, 2H); 7.04 (d, J = 8.38 Hz, 2H); 2.22 (s, 3H). ^{13}C NMR (75 MHz, DMSO- d_6) δ = 158.70, 136.76, 130.90, 128.84 (2xC-Ar); 119.25 (2xC-Ar); 20.36.

1-benzyl-3-hydroxy-urea (**2c**) was obtained as a white powder after purification by reversed-phase chromatography in column 15g, with a gradient from water/acetonitrile (90/10) to acetonitrile 100% (154 mg, 25%). ^1H NMR (300 MHz, DMSO- d_6) δ = 8.63 (bs, 1H); 8.38 (s, 1H); 7.17–7.32 (m, 6H); 4.23 (d, J = 6.34 Hz, 2H). NMR data are in agreement with previously published data [26].

1-hydroxy-3-(4-methoxyphenyl)urea (**2d**) was obtained as a white powder, without further purification (116 mg, 41%). ^1H NMR (300 MHz, DMSO- d_6) δ = 8.85 (d, J = 0.85 Hz, 1H); 8.67 (s, 1H); 8.61 (s, 1H); 7.48 (m, 2H); 6.82 (m, 2H); 3.69 (s, 3H). ^{13}C NMR (75 MHz, DMSO- d_6) δ = 158.85; 154.59; 132.37; 120.87; 113.59; 55.11.

1-(4-fluorophenyl)-3-hydroxy-urea (**2e**) was obtained as a slightly yellow powder, without further purification (366 mg, 82%). ^1H NMR (300 MHz, DMSO- d_6) δ = 8.93 (s, 1H); 8.85 (s, 1H); 8.82 (s, 1H); 7.62 (m, 2H); 7.07 (m, 2H). ^{19}F NMR (300 MHz, DMSO- d_6) δ = -121.3. ^{13}C NMR (75 MHz, DMSO- d_6) δ = 158.70, 157.61 (d, J = 239.22 Hz); 135.78 (d, J = 2.40 Hz); 120.92 (d, J = 7.67 Hz, 2XC-Ar); 114.89 (d, J = 21.90 Hz, 2XC-Ar).

1-(1,3-benzodioxol-5-yl)-3-hydroxy-urea (**2g**) was obtained as a white powder after purification by flash chromatography in column 15g, with a gradient from 100% dichloromethane to 70/30 dichloromethane/ethyl acetate (108 mg, 90%). ^1H NMR (300 MHz, DMSO- d_6) δ = 8.87 (d, J = 0.73 Hz, 1H); 8.72 (s, 1H); 8.66 (s, 1H); 7.28 (d, J = 2.09 Hz, 1H); 7.02 (dd, J = 8.36, 2.09 Hz, 1H); 6.78 (d, J = 8.47 Hz, 1H); 5.94 (s, 2H). ^{13}C NMR (75 MHz, DMSO- d_6) δ = 158.70; 146.88; 142.14; 133.74; 111.95; 107.76; 101.64; 100.70.

1-(3-ethoxypropyl)-3-hydroxy-urea (**2h**) was obtained as a white powder after purification by reversed-phase chromatography in column 15g, with a gradient from water/acetonitrile (90/10) to acetonitrile 100% (194 mg, 82%). ^1H NMR (300 MHz, DMSO- d_6) δ = 8.54 (bs, 1H); 8.22 (s, 1H); 6.68 (s, J = 5.79 Hz, 1H); 3.40 (m, 2H, under solvent peak); 3.09 (q, J = 6.84 Hz, 2H); 1.63 (m, 2H); 1.12–1.07 (t, J = 6.90 Hz, 5H). ^{13}C NMR (75 MHz, DMSO- d_6) δ = 158.88; 67.55; 65.27; 36.52; 30.28; 15.15.

3.1.2. General Procedure for the Synthesis of Hydroxycarbamate Derivatives (3a–k)

In a round-bottom flask, 1.0 eq. of chloroformate was added to a stirred solution of hydroxylamine hydrochloride (2.50 eq.) and sodium hydroxide (3 eq.) in water at room temperature. After 4 h, the mixture was acidified with HCl (1 M) and then extracted three times with ethyl acetate. The organic layer was dried over MgSO_4 and concentrated under reduced pressure to give a crude residue. Purification by flash chromatography afforded the desired compound.

Allyl N-hydroxycarbamate (**3b**) was obtained as a clear oil after purification by flash chromatography in column 15g, with a gradient from 100% cyclohexane to 40/60 cyclohexane/ethyl acetate (93 mg, 95%). ^1H NMR (300 MHz, DMSO- d_6) δ = 9.63 (bs, 1H); 8.71 (s, 1H); 5.89 (m, 1H); 5.22 (m, 2H); 4.50 (dt, J = 5.34, 1.48 Hz). NMR data are in agreement with previously published data [30].

2,2,2-trichloroethyl N-hydroxycarbamate (**3d**) was obtained as a clear oil after purification by flash chromatography in column 15g, with a gradient from 100% cyclohexane to 40/60 cyclohexane/ethyl acetate (373 mg, 71%). ^1H NMR (300 MHz, DMSO- d_6) δ = 10.25 (bs, 1H); 9.01 (s, 1H); 4.82 (s, 2H). ^{13}C NMR (75 MHz, DMSO- d_6) δ = 155.60; 96.08; 73.20.

4-(fluorophenyl) N-hydroxycarbamate (**3e**) was obtained as a white powder, without further purification (337 mg, 86%). ^1H NMR (300 MHz, DMSO- d_6) δ = 10.33 (bs, 1H); 9.08 (s, 1H); 7.11–7.24 (m, 4H). NMR data are in agreement with previously published data [31].

Phenyl N-hydroxycarbamate (**3f**) was obtained as a white powder, without further purification (331 mg, 91%). ^1H NMR (300 MHz, DMSO- d_6) δ = 10.29 (bs, 1H); 9.09 (s, 1H); 7.39 (t, J = 7.73 Hz, 2H); 7.21 (t, J = 7.73 Hz, 1H); 7.10 (d, J = 7.73 Hz, 2H). NMR data are in agreement with previously published data [26].

Isobutyl N-hydroxycarbamate (**3g**) was obtained as a white powder after purification by flash chromatography in column 15g, with a gradient from 100% dichloromethane to 70/30 dichloromethane/ethyl acetate (145 mg, 63%). ^1H NMR (300 MHz, DMSO- d_6) δ = 9.52 (bs, 1H); 8.63 (s, 1H); 3.76 (d, J = 6.72 Hz, 2H); 1.83 (sept, J = 6.59 Hz, 1H); 0.86 (d, J = 6.59 Hz, 6H). ^{13}C NMR (75 MHz, CDCl_3) δ = 158.03; 69.89; 27.65; 18.82 (2xC).

Ethyl N-hydroxycarbamate (**3h**) was obtained as a white powder, without further purification (120 mg, 72%). ^1H NMR (300 MHz, DMSO- d_6) δ = 9.5 (bs, 1H); 8.63 (d, J = 1.24 Hz, 1H); 4.02 (q, J = 7.07 Hz, 2H); 1.15 (t, J = 7.07 Hz, 3H). NMR data are in agreement with previously published data [32].

1,3-benzodioxol-5-yl N-hydroxycarbamate (**3i**) was obtained as a white powder after purification by flash chromatography in column 15g, with a gradient from 100% dichloromethane to 70/30 dichloromethane/ethyl acetate (75 mg, 51%). ^1H NMR (300 MHz, DMSO- d_6) δ = 10.23 (bs, 1H); 9.03 (s, 1H); 6.88 (d, J = 8.29 Hz, 1H); 6.74 (d, 1H, J = 2.42 Hz); 6.54 (dd, 1H, J = 2.42, 8.29 Hz); 6.04 (s, 2H). ^{13}C NMR (75 MHz, DMSO- d_6) δ = 155.70; 147.47; 144.98; 144.46; 113.99; 107.79; 103.92; 101.58.

2-methoxyethyl N-hydroxycarbamate (**3j**) was obtained as an oily white solid, without further purification (230 mg, quant.). ^1H NMR (300 MHz, DMSO- d_6) δ = 9.61 (bs, 1H); 8.67 (d, J = 1.19 Hz, 1H); 4.09 (m, 2H); 3.48 (m, 2H); 3.24 (s, 3H). ^{13}C NMR (75 MHz, DMSO- d_6) δ = 157.71; 70.19; 63.13; 57.96.

Tetrahydropyran-4-yl N-hydroxycarbamate (**3k**) was obtained as a white powder, without further purification (100 mg, 95%). ^1H NMR (300 MHz, DMSO- d_6) δ = 9.56 (bs, 1H); 8.65 (s, 1H); 4.71 (sept, J = 4.29 Hz, 1H); 3.79 (m, 2H); 3.41 (m, 2H); 1.84 (m, 2H); 1.48 (m, 2H). ^{13}C NMR (75 MHz, DMSO- d_6) δ = 157.59; 69.58; 65.09 (2xC); 32.49 (2xC).

3.1.3. General Procedure for the Synthesis of Acylnitroso-Ene Derivatives (4–22)

In a double-neck flask, CuCl (0.05 eq., 1 mg) and pyridine (0.125 eq., 2 μL) were added to the parthenolide (50 mg) and hydroxylamine derivative (1.1 eq.). Then, 2.2 mL of THF was added. The reaction mixture was stirred at room temperature under O_2 (in a balloon). The reaction was monitored using TLC. After 24 h or 48 h, the reaction was stopped with a solution of EDTA (0.5 M, pH 7.0), diluted with ethyl acetate, and stirred until the color no longer persisted in the organic layer. Then, the water phase was extracted three times with ethyl acetate. The organic phase was dried over MgSO_4 and concentrated under reduced pressure to give a crude residue. Purification by flash chromatography afforded the desired compound.

1-hydroxy-1-[(1S,2S,4R,7R,11S)-4-methyl-8,12-dimethylene-13-oxo-3,14-dioxatricyclo [9.3.0.0^{2,4}] tetradecan-7-yl]-3-phenyl-urea (**4**) was obtained as a white powder after purification by flash chromatography in column 4g, with a gradient from 100% dichloromethane to 50/50 dichloromethane/ethyl acetate over 30 min (64 mg, 80%, purity at 254 nm: 100%). ^1H NMR (300 MHz, DMSO- d_6) δ = 9.42 (s, 1H, OH); 8.90 (s, 1H, NH); 7.59 (dd, J = 1.17, 8.76 Hz, 2H, 2 Ar-ortho); 7.23 (t, J = 7.47 Hz, 2H, 2 Ar-meta); 6.96 (m, 1H, Ar-para); 6.03 (d, J = 3.40 Hz, H-11); 5.64 (d, J = 3.12 Hz, 1H, H-11); 5.32 (s, 1H, H-14); 5.08 (s, 1H, H-14); 4.71 (dd, J = 2.84, 11.07 Hz, 1H, H-7); 3.97 (t, J = 9.20 Hz, 1H, H-2); 3.25 (m, 1H, H-1); 2.94 (d, J = 8.51 Hz, 1H, H-3); 2.14–2.38 (m, 5H, H-5, 6, 9, 10); 1.64–1.75 (m, 2H, H-10,6); 1.35 (s, 3H, H-15); 1.07 (t, 1H, H-5). ^{13}C NMR (75 MHz, DMSO- d_6) δ = 169.84 (Cq, C-13); 157.62 (Cq, C-16); 144.81 (Cq, C-12); 140.28 (Cq, C-8); 139.83 (Cq, C-17); 128.84 (CH, 2 C-Ar meta); 122.73 (CH, C-para Ar); 119.80 (CH, 2 C-Ar ortho); 119.61 (CH_2 , C-11); 116.22 (CH_2 , C-14); 80.18 (CH, C-2); 64.20 (CH, C-7); 63.18 (CH, C-3); 60.87 (Cq, C-4); 44.28 (CH, C-1); 36.46

(CH₂, C-5); 29.82 (CH₂, C-9); 26.12 (CH₂, C-6); 25.09 (CH₂, C-10); 18.15 (CH₃, C-15). HRMS (TOF, ES+) *m/z* [M+H]⁺: calcd. for C₂₂H₂₇N₂O₅ 399.1920; found 399.1940.

1-hydroxy-1-[(1S,2S,4R,7R,11S)-4-methyl-8,12-dimethylene-13-oxo-3,14-dioxatricyclo[9.3.0.0^{2,4}]tetradecan-7-yl]-3-(*p*-tolyl)urea (**5**) was obtained as a white powder after purification by flash chromatography in column 4g, with a gradient from 100% dichloromethane to 70/30 dichloromethane/ethyl acetate over 30 min (71 mg, 85%, purity at 254 nm: 96%). ¹H NMR (300 MHz, DMSO-*d*⁶) δ = 9.36 (s, 1H, OH); 8.79 (s, 1H, NH); 7.46 (d, *J* = 8.32 Hz, 2H ortho); 7.03 (d, *J* = 8.13 Hz, 2H meta); 6.03 (d, *J* = 3.43 Hz, 1H, H-11'); 5.64 (d, *J* = 3.09 Hz, 1H, H-11); 5.32 (s, 1H, H-14'); 5.07 (s, 1H, H-14); 4.69 (dd, *J* = 2.83, 11.16 Hz, 1H, H-7); 3.97 (t, *J* = 9.27 Hz, 1H, H-2); 3.25 (m, 1H, H-1); 2.93 (d, *J* = 8.70 Hz, 1H, H-3); 2.13–2.37 (m, 8H, H-5', H-6', H-10', H-9, H-21); 1.64–1.72 (m, 2H, H-10, H-6); 1.35 (s, 3H, H-15); 1.06 (t, *J* = 12.11 Hz, 1H, H-5). ¹³C NMR (75 MHz, DMSO-*d*⁶) δ = 169.39 (Cq, C-13); 157.26 (Cq, C-16); 144.39 (Cq, C-8); 139.84 (Cq, C-12); 136.80 (Cq, C-17); 131.10 (Cq, C-20); 128.80 (CH, C-Ar meta); 119.42 (CH, C-Ar ortho); 119.17 (CH₂, C-11); 115.73 (CH₂, C-14); 79.74 (CH, C-2); 63.79 (CH, C-7); 62.74 (CH, C-3); 60.43 (Cq, C-4); 43.84 (CH, C-1); 36.02 (CH₂, C-5); 29.40 (CH₂, C-9); 25.66 (CH₂, C-6); 24.67 (CH₂, C-10); 20.36 (CH₃, C-21); 17.70 (CH₃, C-15). HRMS (TOF, ES+) *m/z* [M+NH₄]⁺: calcd. for C₂₃H₂₉N₂O₅ 413.2096; found 413.2076.

3-benzyl-1-hydroxy-1-[(1S,2S,4R,7R,11S)-4-methyl-8,12-dimethylene-13-oxo-3,14-dioxatricyclo[9.3.0.0^{2,4}]tetradecan-7-yl]urea (**6**) was obtained as a white powder after purification by flash chromatography in column 4g, with a gradient from 100% dichloromethane to 70/30 dichloromethane/ethyl acetate over 30 min (50 mg, 60%, purity at 254 nm: 100%). ¹H NMR (300 MHz, DMSO-*d*⁶) δ = 9.01 (s, 1H, OH); 7.44 (t, *J* = 6.16 Hz, 1H, NH); 7.17–7.32 (m, 5H, H-Ar); 6.03 (d, *J* = 3.36 Hz, 1H, H-11); 5.65 (d, *J* = 3.17 Hz, 1H, H-11'); 5.27 (s, 1H, H-14); 5.04 (s, 1H, H-14'); 4.58 (dd, *J* = 3.17, 11.38 Hz, 1H, H-7); 4.22 (d, *J* = 6.34 Hz, 2H, H-17); 3.96 (t, *J* = 9.14 Hz, 1H, H-2); 3.24 (m, 1H, H-1); 2.90 (d, *J* = 8.77 Hz, 1H, H-3); 2.11–2.33 (m, 5H, H-5', 6', 9, 9', 10'); 1.61–1.72 (m, 2H, H-6, 10); 1.33 (s, 3H, H-15); 1.02 (t, *J* = 13.07 Hz, 1H, H-5). ¹³C NMR (75 MHz, DMSO-*d*⁶) δ = 169.39 (Cq, C-13); 160.40 (Cq, C-16); 144.53 (Cq, C-8); 140.62 (Cq, C-18); 139.85 (Cq, C-12); 128.07 (CH, 2xC-Ar meta); 127.01 (CH, 2xC-Ar ortho); 126.48 (CH, C-Ar para); 119.16 (CH₂, C-11); 115.48 (CH₂, C-14); 79.75 (CH, C-2); 64.49 (CH, C-7); 62.74 (CH, C-3); 60.44 (Cq, C-4); 43.81 (CH, C-1); 42.84 (CH₂, C-17); 36.05 (CH₂, C-5); 29.47 (CH₂, C-9); 25.50 (CH₂, C-6); 24.67 (CH₂, C-10); 17.69 (CH₃, C-15). HRMS (TOF, ES+) *m/z* [M+H]⁺: calcd. for C₂₃H₂₉N₂O₅ 413.2076; found 413.2081.

1-hydroxy-3-(4-methoxyphenyl)-1-[(1S,2S,4R,7R,11S)-4-methyl-8,12-dimethylene-13-oxo-3,14-dioxatricyclo[9.3.0.0^{2,4}]tetradecan-7-yl]urea (**7**) was obtained as a white powder after purification by flash chromatography in column 4g, with a gradient from 100% dichloromethane to 70/30 dichloromethane/ethyl acetate over 30 min (57 mg, 66%, purity at 254 nm: 99%). ¹H NMR (300 MHz, DMSO-*d*⁶) δ = 9.33 (s, 1H, OH); 8.78 (s, 1H, NH); 7.47 (m, 2H, H-18); 6.81 (m, 2H, H-19); 6.03 (d, *J* = 3.38 Hz, 1H, H-11); 5.64 (d, *J* = 3.11 Hz, 1H, H-11); 5.31 (s, 1H, H-14); 5.07 (s, 1H, H-14); 4.48 (dd, *J* = 3.25, 11.13 Hz, 1H, H-7); 3.97 (t, *J* = 8.77 Hz, 1H, H-2); 3.69 (s, 3H, H-20); 3.24 (m, 1H, H-1); 2.87 (d, *J* = 8.80 Hz, 1H, H-3); 2.11–2.38 (m, 5H, H-9, H-10, H-6, H-5); 1.64–1.73 (m, 2H, H-10, H-6); 1.34 (s, 3H, H-15); 1.06 (t, *J* = 13.37 Hz, 1H, H-5). ¹³C NMR (75 MHz, CDCl₃) δ = 169.44 (Cq, C-13); 157.54 (Cq, C-16); 154.77 (Cq, C-20); 144.44 (Cq, C-8); 139.85 (Cq, C-12); 132.44 (Cq, C-17); 121.12 (CH, C-18); 119.21 (CH₂, C-11); 115.73 (CH₂, C-14); 113.60 (CH, C-19); 79.78 (CH, C-2); 63.93 (CH, C-7); 62.76 (CH, C-3); 60.47 (Cq, C-4); 55.16 (CH₃, C-20); 43.87 (CH, C-1); 36.06 (CH₂, C-5); 29.45 (CH₂, C-9); 25.68 (CH₂, C-6); 24.70 (CH₂, C-10); 17.72 (CH₃, C-15). HRMS (TOF, ES+) *m/z* [M+H]⁺: calcd. for C₂₃H₂₉N₂O₆ 429.2026; found 429.2025.

3-(4-fluorophenyl)-1-hydroxy-1-[(1S,2S,4R,7R,11S)-4-methyl-8,12-dimethylene-13-oxo-3,14-dioxatricyclo[9.3.0.0^{2,4}]tetradecan-7-yl]urea (**8**) was obtained as a white powder after purification by flash chromatography in column 4g, with a gradient from 100% dichloromethane to 70/30 dichloromethane/ethyl acetate over 30 min (46 mg, 55%, purity at 254 nm: 99%). ¹H NMR (300 MHz, DMSO-*d*⁶) δ = 9.41 (s, 1H, OH); 9.01 (s, 1H, NH); 7.61 (m, 2H, H-18); 7.06 (m, 2H, H-19); 6.03 (d, *J* = 3.53 Hz, 1H, H-11'); 5.64 (d, *J* = 3.23 Hz, 1H, H-11); 5.32 (s, 1H, H-14'); 5.08 (s, 1H, H-14); 4.70 (dd, *J* = 2.60, 10.93 Hz, 1H, H-7); 3.97 (t,

J = 9.22 Hz, 1H, H-2); 3.25 (m, 1H, H-1); 2.93 (d, J = 8.80 Hz, 1H, H-3); 2.14–2.38 (m, 5H, H-5', H-6', H-10', 2xH-9); 1.64–1.76 (m, 2H, H-10, H-6); 1.35 (s, 3H, H-15); 1.06 (t, J = 13.27 Hz, 1H, H-5). ^{13}C NMR (75 MHz, DMSO- d_6) δ = 169.39 (Cq, C-13); 159.20 (d, J = 238.68 Hz, Cq, C-20); 157.27 (Cq, C-16); 144.35 (Cq, C-8); 139.83 (Cq, C-12); 135.82 (d, J = 2.42 Hz, Cq, C-17); 121.16 (d, J = 7.63 Hz, CH, C-18); 119.16 (CH₂, C-11); 115.78 (CH₂, C-14); 114.99 (d, J = 21.64 Hz, CH, C-19); 79.73 (CH, C-2); 63.81 (CH, C-7); 62.73 (CH, C-3); 60.42 (Cq, C-4); 43.81 (CH, C-1); 36.99 (CH₂, C-5); 29.35 (CH₂, C-9); 25.66 (CH₂, C-6); 24.63 (CH₂, C-10); 17.70 (CH₃, C-15). HRMS (TOF, ES+) m/z [M+]⁺: calcd. for C₂₂H₂₆FN₂O₅ 417.1826; found 417.1810.

3-(1,3-benzodioxol-5-yl)-1-hydroxy-1-[(1S,2S,4R,7R,11S)-4-methyl-8,12-dimethylene-13-oxo-3,14-dioxatricyclo[9.3.0.0.2,4]tetradecan-7-yl]urea (**10**) was obtained as a white powder after purification by flash chromatography in column 4g, with a gradient from 100% dichloromethane to 70/30 dichloromethane/ethyl acetate over 30 min (30 mg, 34%, purity at 254 nm: 95%). ^1H NMR (300 MHz, DMSO- d_6) δ = 9.36 (s, 1H, OH); 8.83 (s, 1H, NH); 7.27 (d, J = 2.05 Hz, 1H, H-18); 7.02 (dd, J = 2.03, 8.29 Hz, 1H, H-23); 6.77 (d, J = 8.39 Hz, 1H, H-22); 6.03 (d, J = 3.41 Hz, 1H, H-11'); 5.93 (s, 2H, H-20); 5.64 (d, J = 3.05 Hz, 1H, H-11); 5.31 (s, 1H, H-14'); 5.07 (s, 1H, H-14); 4.67 (dd, J = 3.00, 11.57 Hz, 1H, H-7); 3.97 (t, J = 9.06 Hz, 1H, H-2); 3.23 (m, 1H, H-1); 2.93 (d, J = 8.72 Hz, 1H, H-3); 2.11–2.35 (m, 5H, H-5', H-6', H-10', 2xH-9); 1.65–1.72 (m, 2H, H-10, H-6); 1.35 (s, 3H, H-15); 1.06 (t, J = 12.08 Hz, 1H, H-5). ^{13}C NMR (75 MHz, DMSO- d_6) δ = 169.35 (Cq, C-13); 157.28 (Cq, C-16); 146.85 (Cq, C-19); 144.32 (Cq, C-8); 142.25 (Cq, C-21); 139.80 (Cq, C-12); 133.77 (Cq, C-17); 119.12 (CH₂, C-11); 115.70 (CH₂, C-14); 112.14 (CH, C-23); 107.70 (CH, C-22); 101.72 (CH, C-18); 100.71 (CH₂, C-20); 79.72 (CH, C-2); 63.83 (CH, C-7); 62.70 (CH, C-3); 60.39 (Cq, C-4); 43.85 (CH, C-1); 36.01 (CH₂, C-5); 29.41 (CH₂, C-9); 25.63 (CH₂, C-6); 24.66 (CH₂, C-10); 17.67 (CH₃, C-15). HRMS (TOF, ES+) m/z [M+H]⁺: calcd. for C₂₃H₂₇N₂O₇ 443.1818; found 443.1812.

3-(3-ethoxypropyl)-1-hydroxy-1-[(1S,2S,4R,7R,11S)-4-methyl-8,12-dimethylene-13-oxo-3,14-dioxatricyclo[9.3.0.0.2,4]tetradecan-7-yl]urea (**11**) was obtained as a white powder after purification by flash chromatography in column 4g, with a gradient from 100% dichloromethane to 40/50/10 dichloromethane/ethyl acetate/methanol over 30 min (20 mg, 24%, purity at 254 nm: 100%). ^1H NMR (300 MHz, DMSO- d_6) δ = 8.90 (s, 1H, OH); 6.89 (t, J = 5.85 Hz, 1H, NH); 6.02 (d, J = 3.30 Hz, 1H, H-11'); 5.64 (d, J = 3.15 Hz, 1H, H-11); 5.24 (s, 1H, H-14'); 5.03 (s, 1H, H-14); 4.54 (dd, J = 2.36, 10.60 Hz, 1H, H-7); 3.95 (t, J = 9.20 Hz, 1H, H-2); 3.34–3.41 (m, 4H, H-20, H-19); 3.24 (m, 1H, H-1); 3.08 (q, J = 6.71 Hz, 2H, H-17); 2.89 (d, J = 8.57 Hz, 1H, H-3); 2.08–2.37 (m, 5H, H-5', H-6', H-10', 2xH-9); 1.56–1.65 (m, 4H, H-10, H-6, 2xH-18); 1.32 (s, 3H, H-15); 1.07 (m, 4H, H-5, H-21). ^{13}C NMR (75 MHz, DMSO- d_6) δ = 169.35 (Cq, C-13); 160.32 (Cq, C-16); 144.54 (Cq, C-8); 139.80 (Cq, C-12); 119.12 (CH₂, C-11); 115.70 (CH₂, C-14); 79.72 (CH, C-2); 67.98 (CH₂, C-19); 65.29 (CH₂, C-20); 64.37 (CH, C-7); 62.70 (CH, C-3); 60.40 (Cq, C-4); 43.86 (CH, C-1); 37.20 (CH₂, C-17) 36.08 (CH₂, C-5); 29.94 (2xCH₂, C-9, C-18); 25.43 (CH₂, C-6); 24.75 (CH₂, C-10); 17.65 (CH₃, C-15); 15.10 (CH₃, C-21). HRMS (TOF, ES+) m/z [M+H]⁺: calcd. for C₂₁H₃₃N₂O₆ 409.2339; found 409.2329.

tert-butyl-N-hydroxy-N-[(1S,2S,4R,7R,11S)-4-methyl-8,12-dimethylene-13-oxo-3,14-dioxatricyclo[9.3.0.0.2,4]tetradecan-7-yl]carbamate (**12**) was obtained as a white powder after purification by flash chromatography in column 4g, with a gradient from 100% dichloromethane to 70/30 dichloromethane/ethyl acetate over 30 min (42 mg, 55%, purity at 254 nm: 96%). ^1H NMR (300 MHz, DMSO- d_6) δ = 8.95 (s, 1H, OH); 6.03 (d, J = 3.36 Hz, 1H, H-11); 5.65 (d, J = 3.07 Hz, 1H, H-11'); 5.27 (s, 1H, H-14); 5.04 (s, 1H, H-14'); 4.46 (dd, J = 3.07, 10.98 Hz, 1H, H-7); 3.96 (t, J = 9.19 Hz, 1H, H-2); 3.23 (m, 1H, H-3); 2.88 (d, J = 8.77 Hz, 1H, H-1); 2.26–2.39 (m, 2H, H-9, H-10); 2.10–2.20 (m, 3H, H-9', H-6, H-5'); 1.61–1.68 (m, 2H, H-6', H-10'); 1.40 (s, 9H, H-Boc); 1.33 (s, 3H, H-15) 1.02 (t, J = 12.541 Hz, 1H, H-5). ^{13}C NMR (75 MHz, DMSO- d_6) δ = 169.34 (Cq, C-13); 155.40 (Cq, C-16); 144.50 (Cq, C-8); 139.77 (Cq, C-12); 119.18 (CH₂-11); 115.55 (CH₂-14); 79.66 (CH, C-2); 64.56 (CH, C-7); 62.88 (CH, C-1); 60.35 (Cq, C-4); 43.51 (CH, C-3); 35.69 (CH₂, C-5); 28.67 (CH₂, C-9); 28.08 (CH₃-Boc); 25.65 (CH₂, C-6); 24.53 (CH₂, C-10); 17.70 (CH₃-15). Quaternary carbon

C-18 is not shown. HRMS (TOF, ES+) m/z $[M+NH_4]^+$: calcd. for $C_{20}H_{33}N_2O_6$ 397.2339; found 397.2343.

Allyl-N-hydroxy-N-[(1S,2S,4R,7R,11S)-4-methyl-8,12-dimethylene-13-oxo-3,14-dioxatricyclo[9.3.0.02,4]tetradecan-7-yl]carbamate (**13**) was obtained as a white powder after purification by flash chromatography in column 4g, with a gradient from 100% dichloromethane to 70/30 dichloromethane/ethyl acetate over 30 min (37 mg, 50%, purity at 254 nm: 100%). 1H NMR (300 MHz, DMSO- d_6) δ = 9.25 (s, 1H, OH); 6.03 (d, 1H, J = 3.41 Hz, H-11); 5.92 (m, 1H, H-18); 5.62 (d, 1H, J = 3.12 Hz, H-11'); 5.26–5.33 (m, 3H, H-14, 2xH-19); 5.06 (s, 1H, H-14'); 4.52–4.55 (m, 3H, 2xH-17, H-7); 3.96 (t, J = 9.23 Hz, 1H, H-2); 3.24 (m, 1H, H-1); 2.90 (d, J = 8.98 Hz, 1H, H-3); 2.29–2.36 (m, 2H, H-9, H-10); 2.11–2.21 (m, 3H, H-9', H-6, H-5'); 1.64–1.77 (m, 2H, H-6', H-10'); 1.35 (s, 3H, H-15); 1.05 (t, J = 13.08 Hz, 1H H-5). ^{13}C NMR (75 MHz, DMSO- d_6) δ = 169.37 (Cq, C-13); 155.80 (Cq, C-16); 144.23 (Cq, C-8); 139.79 (Cq, C-12); 133.23 (CH, C-18); 119.15 (CH₂, C-11); 117.45 (CH₂, C-19); 115.98 (CH₂, C-14); 79.64 (CH, C-2); 65.48 (CH, C-17); 64.67 (Cq, C-7); 62.82 (CH, C-3); 60.34 (Cq, C-4); 43.49 (CH, C-1); 35.58 (CH₂, C-5); 28.60 (CH₂, C-9); 25.59 (CH₂, C-6); 24.35 (CH₂, C-10); 17.71 (CH₃, C-15). HRMS (TOF, ES+) m/z $[M+H]^+$: calcd. for $C_{19}H_{26}NO_6$ 364.1760; found 364.1773.

Benzyl-N-hydroxy-N-[(1S,2S,4R,7R,11S)-4-methyl-8,12-dimethylene-13-oxo-3,14-dioxatricyclo[9.3.0.02,4]tetradecan-7-yl]carbamate (**14**) was obtained as a white powder after purification by flash chromatography in column 4g, with a gradient from 100% dichloromethane to 70/30 dichloromethane/ethyl acetate over 30 min (64 mg, 77%, purity at 254 nm: 98%). 1H NMR (300 MHz, DMSO- d_6) δ = 9.27 (s, 1H, OH); 7.31–7.38 (m, 5H-Ar); 6.03 (d, J = 3.43 Hz, 1H, H-11); 5.64 (d, J = 3.05 Hz, 1H, H-11); 5.29 (s, 1H, H-14); 5.09 (d, J = 3.15 Hz, 2H, H-17); 5.06 (s, 1H, H-14); 4.56 (dd, J = 3.05, 10.88 Hz, H-7); 3.96 (t, J = 9.24 Hz, 1H, H-2); 3.22 (m, 1H, H-1); 2.89 (d, J = 8.87 Hz, 1H, H-3); 2.29–2.36 (m, 2H, H-9, H-10); 2.11–2.20 (m, 3H, H-6, H-5, H-9); 1.63–1.71 (m, 2H, H-6, H-10); 1.34 (s, 3H, H-15); 1.05 (t, J = 12.57 Hz, 1H, H-5). ^{13}C NMR (75 MHz, DMSO- d_6) δ = 169.36 (Cq, C-13); 155.95 (Cq, C-16); 144.21 (Cq, C-8); 139.78 (Cq, C-12); 136.62 (Cq, C-18); 128.39 (CH, 2 C-Ar); 127.98 (CH, C-para Ar); 127.89 (CH, 2 C-Ar); 119.17 (CH₂, C-11); 116.03 (CH₂, C-14); 79.64 (CH, C-2); 66.46 (CH₂, C-17); 64.66 (CH, C-7); 62.82 (CH, C-3); 60.33 (Cq, C-4); 43.44 (CH, C-1); 35.57 (CH₂, C-5); 28.59 (CH₂, C-9); 25.59 (CH₂, C-6); 24.43 (CH₂, C-10); 17.70 (CH₃, C-15). HRMS (TOF, ES+) m/z $[M+NH_4]^+$: calcd. for $C_{23}H_{31}N_2O_6$ 431.2182; found 431.2187.

2,2,2-trichloroethyl-N-hydroxy-N-[(1S,2S,4R,7R,11S)-4-methyl-8,12-dimethylene-13-oxo-3,14-dioxatricyclo[9.3.0.02,4]tetradecan-7-yl]carbamate (**15**) was obtained as a white powder after purification by flash chromatography in column 4g, with a gradient from 100% dichloromethane to 80/20 dichloromethane/ethyl acetate over 30 min (55 mg, 60%, purity at 215 nm: 100%). 1H NMR (300 MHz, DMSO- d_6) δ = 9.60 (s, 1H, OH); 6.03 (d, J = 3.44 Hz, 1H, H-11); 5.66 (d, J = 3.17 Hz, 1H, H-11); 5.35 (s, 1H, H-14); 5.12 (s, 1H, H-14); 4.88 (m, 2H, H-17); 4.59 (dd, J = 3.07 Hz, 1H, H-7); 3.98 (t, J = 9.10 Hz, 1H, H-2); 3.22 (m, 1H, H-1); 2.90 (d, J = 8.91 Hz, 1H, H-3); 2.13–2.35 (m, 5H, H-5, H-6, H-9, H-10); 1.65–1.76 (m, 2H, H-6, H-10); 1.34 (s, 3H, H-15); 1.05 (t, J = 12.63 Hz, 1H, H-5). ^{13}C NMR (75 MHz, DMSO- d_6) δ = 169.80 (Cq, C-13); 154.35 (Cq, C-16); 144.13 (Cq, C-12); 140.19 (Cq, C-8); 119.72 (CH₂, C-11); 116.96 (CH₂, C-14); 96.25 (Cq, C-16); 80.10 (CH, C-2); 74.60 (CH₂, C-17); 65.52 (CH, C-7); 63.31 (CH, C-3); 60.75 (Cq, C-4); 44.08 (CH, C-1); 36.07 (CH₂, C-5); 29.15 (CH₂, C-9); 26.02 (CH₂, C-6); 25.15 (CH₂, C-10); 18.12 (CH₃, C-15). HRMS (TOF, ES+) m/z $[M+H]^+$: calcd. for $C_{18}H_{23}Cl_3NO_6$ 454.0584; found 454.0591.

(4-fluorophenyl)-N-hydroxy-N-[(1S,2S,4R,7R,11S)-4-methyl-8,12-dimethylene-13-oxo-3,14-dioxatricyclo[9.3.0.02,4]tetradecan-7-yl]carbamate (**16**) was obtained as a slightly yellow powder after purification by flash chromatography in column 4g, with a gradient from 100% dichloromethane to 70/30 dichloromethane/ethyl acetate over 30 min (28 mg, 33%, purity at 254 nm: 98%). 1H NMR (300 MHz, DMSO- d_6) δ = 9.67 (s, 1H); 7.11–7.25 (m, 4H, H-Ar); 6.04 (d, J = 3.50 Hz, 1H, H-11); 5.66 (d, J = 3.22 Hz, 1H, H-11'); 5.38 (s, 1H, H-14); 5.15 (s, 1H, H-14'); 4.63 (dd, J = 3.01, 11.46 Hz, 1H, H-7); 3.98 (t, J = 9.06 Hz, 1H, H-2); 3.25 (m, 1H, H-1); 2.93 (d, J = 8.93 Hz, 1H, H-3); 2.15–2.42 (m, 5H, H-5, H-6, H-10, H-9); 1.67–1.84

(m, 2H, H-6', H-10'); 1.36 (s, 3H, H-15); 1.10 (t, J = 12.62 Hz, 1H, H-5'). ¹³C NMR (75 MHz, DMSO-d⁶) δ = 169.38 (Cq, C-13); 159.29 (d, J = 241.78 Hz, Cq, C-20); 147.06 (d, J = 2.99 Hz, Cq, C-17); 143.90 (Cq, C-8); 139.77 (Cq, C-12); 123.51 (d, J = 8.78 Hz, 2xCH, C-18); 119.17 (CH₂, C-11); 116.39 (CH₂, C-14); 115.95 (d, J = 23.10 Hz, 2xCH, C-19); 79.61 (CH, C-2); 65.04 (CH, C-7); 62.70 (CH, C-3); 60.34 (Cq, C-4); 43.64 (CH, C-1); 35.53 (CH₂, C-5); 28.63 (CH₂, C-9); 25.60 (CH₂, C-6); 24.29 (CH₂, C-10); 17.69 (CH₃, C-15). HRMS (TOF, ES+) *m/z* [M+H]⁺: calcd. for C₂₂H₂₅FNO₆ 418.1654; found 418.1666.

Phenyl-N-hydroxy-N-[(1S,2S,4R,7R,11S)-4-methyl-8,12-dimethylene-13-oxo-3,14-dioxatricyclo[9.3.0.02,4]tetradecan-7-yl]carbamate (**17**) was obtained as a white powder after purification by flash chromatography in column 4g, with a gradient from 100% dichloromethane to 80/20 dichloromethane/ethyl acetate over 30 min (37 mg, 45%, purity at 254 nm: 99%). ¹H NMR (300 MHz, DMSO-d⁶) δ = 9.64 (s, 1H, OH); 7.40 (m, 2H, H-18); 7.23 (m, 1H, H-20); 7.09 (m, 2H, H-19); 6.03 (d, J = 3.44 Hz, 1H, H-11'); 5.66 (d, J = 3.13 Hz, 1H, H-11); 5.38 (s, 1H, H-14'); 5.15 (s, 1H, H-14); 4.64 (dd, J = 3.06, 11.38 Hz, 1H, H-7); 3.98 (t, J = 9.08 Hz, 1H, H-2); 3.26 (m, 1H, H-1); 2.93 (d, J = 9.08 Hz, 1H, H-3); 2.15–2.43 (m, 5H, H-5', H-6', H-10', H-9); 1.65–1.84 (m, 2H, H-10, H-6); 1.36 (s, 3H, H-15); 1.11 (t, J = 12.49 Hz, 1H, H-5). ¹³C NMR (75 MHz, DMSO-d⁶) δ = 169.37 (Cq, C-13); 154.06 (Cq, C-16); 151.00 (Cq, C-17) 143.97 (Cq, C-8); 139.78 (Cq, C-12); 129.40 (2xCH, C-18); 125.36 (CH, C-20); 121.70 (2xCH, C-19); 119.16 (CH₂, C-11); 116.35 (CH₂, C-14); 79.61 (CH, C-2); 65.01 (CH, C-7); 62.71 (CH, C-3); 60.34 (Cq, C-4); 43.60 (CH, C-1); 35.53 (CH₂, C-5); 28.61 (CH₂, C-9); 25.62 (CH₂, C-6); 24.27 (CH₂, C-10); 17.69 (CH₃, C-15). HRMS (TOF, ES+) *m/z* [M+H]⁺: calcd. for C₂₂H₂₆NO 400.1760; found 400.1747.

Isobutyl-N-hydroxy-N-[(1S,2S,4R,7R,11S)-4-methyl-8,12-dimethylene-13-oxo-3,14-dioxatricyclo[9.3.0.02,4]tetradecan-7-yl]carbamate (**18**) was obtained as a white powder after purification by flash chromatography in column 4g, with a gradient from 100% dichloromethane to 70/30 dichloromethane/ethyl acetate over 30 min (50 mg, 65%, purity at 215 nm: 98%). ¹H NMR (300 MHz, DMSO-d⁶) δ = 9.16 (s, 1H, OH); 6.03 (d, J = 3.39 Hz, 1H, H-11); 5.65 (d, J = 3.13 Hz, 1H, H-11); 5.28 (s, 1H, H-14); 5.06 (s, 1H, H-14); 4.51 (dd, J = 2.90, 10.90 Hz, H-7); 3.97 (t, J = 9.16 Hz, 1H, H-2); 3.79 (d, J = 6.03 Hz, 2H, H-17); 3.23 (m, 1H, H-1); 2.89 (d, J = 8.93 Hz, 1H, H-3); 2.29–2.38 (m, 2H, H-9, H-10); 2.11–2.23 (m, 3H, H-6, H-5, H-9); 1.85 (m, 1H, H-18); 1.64–1.71 (m, 2H, H-6, H-10); 1.34 (s, 3H, H-15); 1.04 (t, J = 12.32 Hz, 1H, H-5); 0.87 (d, J = 6.67 Hz, 6H, H-19, H-20). ¹³C NMR (75 MHz, DMSO-d⁶) δ = 169.83 (Cq, C-13); 156.72 (Cq, C-16); 144.75 (Cq, C-8); 140.22 (Cq, C-12); 119.64 (CH₂, C-11); 116.34 (CH₂, C-14); 80.10 (CH, C-2); 71.40 (CH₂, C-17) 65.18 (CH, C-7); 63.32 (CH, C-3); 60.80 (Cq, C-4); 43.93 (CH, C-1); 36.06 (CH₂, C-5); 29.05 (CH₂, C-9); 28.03 (CH, C-18); 26.06 (CH₂, C-6); 24.88 (CH₂, C-10); 19.32 (CH₃, C-19, C-20); 18.15 (CH₃, C-15). HRMS (TOF, ES+) *m/z* [M+H]⁺: calcd. for C₂₀H₃₀NO₆ 380.2073; found 380.2045.

Ethyl-N-hydroxy-N-[(1S,2S,4R,7R,11S)-4-methyl-8,12-dimethylene-13-oxo-3,14-dioxatricyclo[9.3.0.02,4]tetradecan-7-yl]carbamate (**19**) was obtained as a white powder after purification by flash chromatography in column 4g, with a gradient from 100% dichloromethane to 60/40 dichloromethane/ethyl acetate over 30 min (30 mg, 42%, purity at 254 nm: 98%). ¹H NMR (300 MHz, DMSO-d⁶) δ = 9.17 (s, 1H, OH); 6.02 (d, J = 3.40 Hz, 1H, H-11); 5.64 (d, J = 3.14 Hz, 1H, H-11'); 5.28 (s, 1H, H-14); 5.05 (s, 1H, H-14'); 4.51 (dd, J = 2.99, 10.85 Hz, 1H, H-7); 3.93–4.08 (m, 3H, H-2, 2xH-17); 3.23 (m, 1H, H-1); 2.89 (d, J = 8.89 Hz, H-3); 2.28–2.38 (m, 2H, H-9, H-10); 2.08–2.21 (m, 3H, H-6, H-5, H-9'); 1.63–1.70 (m, 2H, H-6', H-10'); 1.33 (s, 3H, H-15); 1.17 (t, J = 7.09 Hz, 3H, H-18); 1.04 (t, J = 12.66 Hz, 1H, H-5'). ¹³C NMR (75 MHz, DMSO-d⁶) δ = 169.47 (Cq, C-13); 156.30 (Cq, C-16); 144.35 (Cq, C-8); 139.83 (Cq, C-12); 119.25 (CH₂, C-11); 115.95 (CH₂, C-14); 79.73 (CH, C-2); 64.64 (CH, C-7); 62.90 (CH, C-3); 61.10 (CH₂-C-17); 60.43 (Cq, C-4); 43.53 (CH, C-1); 35.65 (CH₂, C-5); 28.66 (CH₂, C-9); 25.64 (CH₂, C-6); 24.42 (CH₂, C-10); 17.76 (CH₃, C-15); 14.65 (CH₃, C-18). HRMS (TOF, ES+) *m/z* [M+H]⁺: calcd. for C₁₈H₂₆NO₆ 352.1760; found 352.1764.

1,3-benzodioxol-5-yl-N-hydroxy-N-[(1S,2S,4R,7R,11S)-4-methyl-8,12-dimethylene-13-oxo-3,14-dioxatricyclo[9.3.0.02,4]tetradecan-7-yl]carbamate (**20**) was obtained as a white powder after purification by flash chromatography in column 4g, with a gradient from

100% dichloromethane to 80/20 dichloromethane/ethyl acetate over 30 min (37 mg, 41%, purity at 254 nm: 96%). ^1H NMR (300 MHz, DMSO- d_6) δ = 9.61 (s, 1H, OH); 6.88 (d, 1H, J = 8.46 Hz, H-22); 6.73 (d, 1H, J = 2.37 Hz, H-18); 6.53 (dd, 1H, J = 2.37, 8.46 Hz, H-21); 6.02–6.05 (m, 3 H, H-20, H-11); 5.66 (d, 1H, J = 3.47 Hz, H-11'); 5.37 (s, 1H, H-14); 5.14 (s, 1H, 14'); 4.60 (dd, 1H, J = 10.94, 2.43 Hz, H-7); 3.97 (t, 1H, J = 8.99 Hz, H-2); 3.25 (m, 1H, H-1); 2.90 (d, 1H, J = 8.76 Hz, H-3); 2.13–2.43 (m, 5H, H-9, H-9', H-10, H-6, H-5); 1.65–1.85 (m, 2H, H-10', H-6'); 1.36 (s, 3H, H-15); 1.10 (m, 1H, H-5'). ^{13}C NMR (75 MHz, DMSO- d_6) δ = 169.38 (Cq, C-13); 154.27 (Cq, C-16); 147.49 (Cq, C-19); 145.29 (Cq, C-17); 144.61 (Cq, C-21); 143.93 (Cq, C-8); 139.78 (Cq, C-12); 119.17 (CH₂, C-11); 116.34 (CH₂, C-14); 114.09 (CH, C-23); 107.82 (CH, C-22); 103.94 (CH, C-18); 101.66 (CH₂, C-20); 79.02 (CH, C-2); 65.01 (CH, C-7); 62.70 (CH, C-3); 60.35 (Cq, C-4); 43.62 (CH, C-1); 35.53 (CH₂, C-5); 28.63 (CH₂, C-9); 25.60 (CH₂, C-6); 24.28 (CH₂, C-10); 17.69 (CH₃, C-15). HRMS (TOF, ES+) m/z [M+H]⁺: calcd. for C₂₃H₂₆NO₈ 444.1658; found 444.1629.

2-methoxyethyl-N-hydroxy-N-[(1S,2S,4R,7R,11S)-4-methyl-8,12-dimethylene-13-oxo-3,14-dioxatricyclo[9.3.0.02,4]tetradecan-7-yl]carbamate (**21**) was obtained as a white powder after purification by flash chromatography in column 4g, with a gradient from 100% dichloromethane to 70/30 dichloromethane/ethyl acetate over 30 min (30 mg, 40%, purity at 254 nm: 99%). ^1H NMR (300 MHz, DMSO- d_6) δ = 9.23 (s, 1H, OH); 6.03 (d, J = 3.45 Hz, 1H, H-11); 5.65 (d, J = 3.06 Hz, 1H, H-11'); 5.29 (s, 1H, H-14); 5.06 (s, 1H, H-14'); 4.51 (dd, J = 2.87, 10.52 Hz, 1H, H-7); 4.11 (m, 2H, H-17) 3.97 (t, J = 9.18 Hz, H-2); 3.50 (t, J = 4.78 Hz, 2H, H-18); 3.22–3.26 (m, 4H, H-1, H-19); 2.89 (d, J = 8.99 Hz, H-3); 2.28–2.38 (m, 2H, H-9, H-10); 2.08–2.21 (m, 3H, H-6, H-5, H-9'); 1.63–1.73 (m, 2H, H-6', H-10'); 1.34 (s, 3H, H-15); 1.04 (t, J = 12.63 Hz, 1H, H-5'). ^{13}C NMR (75 MHz, DMSO- d_6) δ = 169.83 (Cq, C-13); 156.55 (Cq, C-16); 144.76 (Cq, C-8); 140.24 (Cq, C-12); 119.66 (CH₂, C-11); 116.36 (CH₂, C-14); 80.16 (CH, C-2); 70.55 (CH₂, C-18); 64.96 (CH, C-7); 64.65 (CH₂, C-17); 63.34 (CH, C-3); 60.79 (Cq, C-4); 58.46 (CH₃, C-19); 43.87 (CH, C-1); 36.06 (CH₂, C-5); 29.06 (CH₂, C-9); 26.01 (CH₂, C-6); 25.06 (CH₂, C-10); 18.17 (CH₃, C-15). HRMS (TOF, ES+) m/z [M+H]⁺: calcd. for C₁₉H₂₈NO₇ 382.1866; found 382.1875.

Tetrahydropyran-4-yl-N-hydroxy-N-[(1S,2S,4R,7R,11S)-4-methyl-8,12-dimethylene-13-oxo-3,14-dioxatricyclo[9.3.0.02,4]tetradecan-7-yl]carbamate (**22**) was obtained as a white powder after purification by flash chromatography in column 4g, with a gradient from 100% dichloromethane to 70/30 dichloromethane/ethyl acetate over 30 min (52 mg, 63%, purity at 254 nm: 95%). ^1H NMR (300 MHz, DMSO- d_6) δ = 9.18 (s, 1H, OH); 6.03 (d, J = 3.47 Hz, 1H, H-11); 5.65 (d, J = 3.16 Hz, 1H, H-11'); 5.28 (s, 1H, H-14); 5.05 (s, 1H, H-14'); 4.73 (m, 1H, H-17); 4.52 (dd, J = 3.00, 10.75 Hz, 1H, H-7); 3.97 (t, J = 9.17 Hz, 1H, H-2); 3.79 (m, 2H, H-19); 3.42 (m, 2H, H-20 under water peak); 3.23 (m, 1H, H-1); 2.89 (d, J = 9.01 Hz, H-3); 2.11–2.38 (m, 5H, H-6, H-5, 2xH-9, H-10); 1.84 (m, 2H, H-18); 1.63–1.70 (m, 2H, H-6', H-10'); 1.52 (m, 2H, H-21); 1.33 (s, 3H, H-15); 1.04 (t, J = 14.57 Hz, 1H, H-5'). ^{13}C NMR (75 MHz, DMSO- d_6) δ = 169.83 (Cq, C-13); 155.92 (Cq, C-16); 144.73 (Cq, C-8); 140.23 (Cq, C-12); 119.65 (CH₂, C-11); 116.33 (CH₂, C-14); 80.10 (CH, C-2); 70.62 (CH, C-17); 65.08 (CH, C-7); 64.99 (2xCH₂, C-19, C-20); 63.32 (CH, C-3); 60.81 (Cq, C-4); 43.96 (CH, C-1); 36.05 (CH₂, C-5); 32.36 (2xCH₂, C-18, C-21); 29.08 (CH₂, C-9); 26.08 (CH₂, C-6); 24.90 (CH₂, C-10); 18.16 (CH₃, C-15). HRMS (TOF, ES+) m/z [M+NH₄]⁺: calcd. for C₂₁H₃₃N₂O₇ 425.2288; found 425.2279.

3.1.4. Synthesis of 1-hydroxy-1-[1S,2S,4R,7R,11S)-4-methyl-8,12-dimethylene-13-oxo-3,14-dioxatricyclo[9.3.0.02,4]tetradecan-7-yl]urea (**9**)

In a double-neck flask, CuCl (0.05 eq., 1 mg) and pyridine (0.125 eq., 2 μL) were added to the parthenolide (50 mg) and hydroxylamine derivative (1.1 eq.). Then, 2.2 mL of THF was added. The reaction mixture was stirred at room temperature while being exposed to the air. The reaction was monitored using TLC. After 24 h or 48 h, the reaction was stopped with a solution of EDTA (0.5 M, pH 7.0), diluted with ethyl acetate, and stirred until the color no longer persisted in the organic layer. Then, the water phase was extracted three times with ethyl acetate. The organic phase was dried over MgSO₄ and concentrated under

reduced pressure to give a crude residue. Purification by reversed-phase chromatography in column 15g, with a gradient from water/acetonitrile (90/10) to acetonitrile (100%) over 30 min afforded the desired compound (9) as a white powder (59 mg, 91%, purity at 254 nm: 99%). ^1H NMR (300 MHz, DMSO- d_6) δ = 8.97 (s, 1H, OH); 6.28 (s, 2H, NH₂); 6.03 (d, J = 3.42 Hz, 1H, H-11); 5.64 (d, J = 3.11 Hz, 1H); 5.26 (s, 1H, H-14); 5.03 (s, 1H, H-14); 4.57 (dd, J = 2.63, 11.23 Hz, 1H, H-7); 3.95 (t, J = 9.41 Hz, 1H, H-2); 3.23 (m, 1H, H-1); 2.90 (d, J = 8.89 Hz, 1H, H-3); 2.23–2.33 (m, 3H, 2xH-9, H-10); 2.04–2.20 (m, 2H, H-5, H-6) 1.57–1.71 (m, 2H, H-6, H-10); 1.32 (s, 3H, H-15); 1.00 (t, J = 12.97 Hz, 1H, H-5). ^{13}C NMR (75 MHz, DMSO- d_6) δ = 169.41 (Cq, C-13); 161.18 (Cq, C-16); 144.65 (Cq, C-8); 139.86 (Cq, C-12); 119.16 (CH₂, C-11); 115.30 (CH₂, C-14); 79.76 (CH, C-2); 63.52 (CH, C-7); 62.72 (CH, C-3); 60.46 (Cq, C-4); 43.93 (CH, C-1); 35.10 (CH₂, C-5); 28.50 (CH₂, C-9); 25.51 (CH₂, C-6); 24.78 (CH₂, C-10); 17.68 (CH₃, C-15). HRMS (TOF, ES+) m/z [M+H]⁺: calcd. for C₁₆H₂₃N₂O₅ 323.1607; found 323.1610.

3.1.5. Synthesis of (1S,2S,4R,7Z,11S)-7-hydroxyimino-4-methyl-8,12-dimethylene-3,14-dioxatricyclo[9.3.0.0^{2,4}] tetradecan-13-one (23)

In a double-neck flask, CuCl (0.05 eq., 1 mg) and pyridine (0.125 eq., 2 μL) were added to the parthenolide (50 mg) and hydroxylamine derivative (1.1 eq.). Then, 2.2 mL of THF was added. The reaction mixture was stirred at room temperature under O₂ (in a balloon). The reaction was monitored using TLC. After 24 h or 48 h, the reaction was stopped with a solution of EDTA (0.5 M, pH 7.0), diluted with ethyl acetate, and stirred until the color no longer persisted in the organic layer. Then, the water phase was extracted three times with ethyl acetate. The organic phase was dried over MgSO₄ and concentrated under reduced pressure to give a crude residue. Purification by reversed-phase chromatography in column 4g, with a gradient from water/acetonitrile (90/10) to acetonitrile (100%) over 30 min afforded the desired compound (23) as a white powder (10 mg, 18%, purity at 254 nm: 99%). ^1H NMR (300 MHz, DMSO- d_6) δ = 11.30 (s, OH); 6.09 (d, J = 3.67 Hz, 1H, H-11); 5.76 (d, J = 3.36 Hz, 1H, H-11') 5.48 (s, 1H, H-14'); 5.39 (s, 1H, H-14); 3.92 (t, J = 9.34 Hz, 1H, H-2); 2.87–3.02 (m, 2H, H-1, H-10); 2.55–2.70 (m, 3H, H-3, H-9, H-10'); 2.45 (m, 1H, H-9'); 2.05–2.18 (m, 2H, H-5, H-6); 1.47–1.61 (m, 2H, H-6', H-5'); 1.26 (s, 3H, H-15). ^{13}C NMR (75 MHz, DMSO- d_6) δ = 169.28 (Cq, C-13); 156.24 (Cq, C-16); 145.00 (Cq, C-8); 139.83 (Cq, C-12); 119.67 (CH₂, C-11); 118.11 (CH₂, C-14); 81.59 (CH, C-2); 64.04 (CH, C-3); 60.06 (Cq, C-4); 44.14 (CH, C-1); 32.95 (CH₂, C-5); 32.25 (CH₂, C-9); 28.55 (CH₂, C-6); 19.56 (CH₂, C-10); 17.22 (CH₃, C-15). HRMS (TOF, ES+) m/z [M+H]⁺: calcd. for C₁₅H₂₀NO₄ 278.1392; found 278.1408.

3.1.6. Synthesis of (1S,2S,4R,7E,11S)-4,8,12-trimethyl-3,14-dioxatricyclo[9.3.0.0^{2,4}]tetradec-7-en-13-one (26)

In an assay tube, parthenolide (100 mg) was diluted in 8 mL of methanol (0.05 M). The reaction was performed in a H-Cube with a Pd/C cartridge at r.t. in the full H₂ mode. Three runs were necessary to obtain the full conversion of the parthenolide. The reaction led to the formation of 2 diastereomers. Major diastereomers: 70%; minor diastereomers: 30% (101 mg, 61%, purity at 254 nm: 97%). ^1H NMR (300 MHz, CDCl₃) δ = 5.17 (dd, J = 2.53 Hz, 1H); 3.81 (t, J = 9.12 Hz, 1H); 2.70 (d, J = 9.12 Hz, 1H); 2.25–2.42 (m, 3H); 2.09–2.19 (m, 2H); 2.04 (m, 1H); 1.79–1.93 (m, 2H); 1.59–1.70 (m, 8H); 1.11–1.29 (m, 8H).

3.2. Biological Evaluation

3.2.1. Strains and Growth Conditions

The *Mycobacterium tuberculosis* strain H37Rv expressing GFP, H37Rv::pJKD6, was generated as described previously (DOI:10.1128/AEM.03677-15) and cultured in Middlebrook 7H9 medium supplemented with 10% OADC, 0.2% glycerol, 0.05% Tween[®] 80, and 20 $\mu\text{g}/\text{mL}$ kanamycin (for maintaining selection on pJKD6). *Staphylococcus aureus* (SH1000) was kindly provided by Simon J. Foster (the University of Sheffield) and grown in cation-adjusted Mueller Hinton II broth.

3.2.2. Determination of MICs

The minimal inhibitory concentrations (MICs) of the compounds against *M. tuberculosis* were determined using both GFP and resazurin (REMA) as a readout of the bacterial viability. Briefly, a mid-log phase of the H37Rv::pJKD6 cultures was diluted to an OD₆₀₀ of 0.001 and distributed in a 96-well plate (100 µL) in the presence of serial dilutions of the compounds of interest. Following 7 days of incubation (at 37 °C), bacterial growth was measured based on GFP fluorescence (Ex. at 485 nm; Em. at 510 nm) using an EnSight fluorescence plate reader (Perkin Elmer). Subsequently, 10 µL of resazurin (0.1% w/v) was added to the same bacteria and incubated (for 18 h at 37 °C), and the bacterial metabolic conversion of resazurin to resorufin was measured based on fluorescence (Ex. at 560 nm; Em. at 590 nm) using the same plate reader. For the GFP fluorescence readout, the data were background-corrected (without a bacterial control) and expressed as a percentage of the GFP signal compared to that for the untreated bacteria, with MIC GFP defined as the concentration that results in less than 2% of the initial GFP signal. For the resazurin (REMA) fluorescence readout, the data were background-corrected (without a bacterial control) and expressed as a percentage of the REMA signal compared to that for the untreated bacteria, with MIC REMA defined as the concentration that results in less than 10% of the initial REMA signal.

The MICs of the compounds against *S. aureus* were determined using only the resazurin (REMA)-based viability readout. The experiment was performed as for *M. tuberculosis*, with the following changes: the bacteria were grown in the presence of the compounds for only 5 h (not 7 days) and were co-incubated with resazurin for 1 h before the fluorescence reading and analysis.

3.2.3. X-ray Structural Determination

Single-crystal X-ray crystallographic analyses were conducted on compound **14**. The diffraction data were obtained using a combination of phi- and omega-scans on a Bruker Apex DUO diffractometer equipped with a Photon 3 hybrid pixel area detector mounted on a four-circle D8 goniometer. Cu K α radiation ($\lambda = 1.54178 \text{ \AA}$) was obtained using an ImuS Incoatec Cu microfocus sealed tube. The data solution was found using SHELXT [33] and refined using SHELXL [34], as implemented in the Olex 2 crystallographic suite for small molecules [35]. The X-ray crystallographic data for compound **14** have been deposited at the Cambridge Crystallographic Data Centre, under the reference number CCDC-2226330, and can be obtained freely at <https://www.ccdc.cam.ac.uk/structures/> (accessed on 11 December 2023).

3.2.4. Solubility Determination

The kinetic solubility was determined using LC–MS/MS analysis in PBS at pH 7.4. Briefly, a 10 mM 100% DMSO solution of the compound was diluted 50-fold either in PBS at pH 7.4 (in triplicate) or in DMSO in polypropylene tubes ($n = 3$ for PBS and $n = 6$ for DMSO). The tubes were gently shaken for 24 h at 21 °C. Then, the three PBS tubes and three of the six DMSO tubes were centrifuged for 5 min at 4000 rpm and filtered over 0.45 µm filters (Millex-LH Millipore). Then, 40 µL of each solution was diluted in 160 µL of MeCN and 40 µL of Milli-Q water and transferred to matrix tubes for the LC–MS/MS analysis. The solubility was determined according to the following formula: Solubility (µM) = (AUC (filtered PBS)/AUC (not filtered DMSO)) \times 200. The test was validated if (AUC (not filtered DMSO) – AUC (filtered DMSO))/AUC (not filtered DMSO) \leq 10%.

3.2.5. Cytotoxicity

The cytotoxicity of the compounds to BALB/3T3 cells was determined using live imaging following both Hoechst 33342 and propidium iodide staining. Briefly, BALB/3T3 cells were seeded in a 384-well plate and 24 h later, the compounds were added (0, 12.5, 25, 50, and 100 µM) to the culture medium, as well as Hoechst 33342 and propidium iodide (PI). Then, 24 h and 48 h after the compounds were added, live imaging was performed using

an In Cell Analyzer 6000 (STP GE Healthcare, Glasgow, UK). The cytotoxicity was defined based on the ratio of the population of dead or dying cells (propidium iodide staining) to the total cell population (Hoechst staining), as determined using Columbus software 2.9.1 (PerkinElmer Informatics, WA, USA). The compounds were tested in triplicate. Carfilzomib (500, 250, 140, and 60 nM) was used as the positive control in this assay.

4. Conclusions

In this study, we described the regioselective and stereoselective acylnitroso-ene modification of parthenolide, which provided 19 original compounds that were screened for their antibacterial activities. The reaction proceeded through the Markovnikov addition of an electron-deficient enophile, nitroso species, to an ene, parthenolide. To the best of our knowledge, the mechanism of this reaction has not been fully elucidated yet. Therefore, according to our crystallographic and NOESY data, we were able to suggest a mechanism to explain the regioselectivity and stereoselectivity. Two series of compounds, ureas and carbamates, bearing aromatic and alkyl groups, were synthesized in moderate to good yields. All the compounds were tested against *M. tuberculosis* and *S. aureus*, and *M. tuberculosis*-specific antibacterial activity was found. It should also be noted that the Michael acceptor is necessary for the activity, but further studies are necessary to fully understand how nitroso-ene derivatives inhibit *M. tuberculosis* growth. Advantageously, nitroso-ene derivatives are more water soluble than parthenolide while maintaining activity against *M. tuberculosis*.

Supplementary Materials: The following supporting information can be downloaded at <https://www.mdpi.com/article/10.3390/ijms242417395/s1>.

Author Contributions: Conceptualization, N.W. and B.G.; methodology, B.G., A.B., V.L., P.R. and C.P.; validation, B.G., F.R. and R.C.H.; formal analysis, B.G.; resources, N.W. and R.C.H.; data curation, B.G. and F.L.; writing—original draft preparation, B.G. and N.W.; writing—review and editing, B.G., N.W. and F.R.; supervision, N.W.; funding acquisition, N.W. All authors have read and agreed to the published version of the manuscript.

Funding: The Chevreul Institute (FR CNRS 2638) is funded by the “Ministère de l’Enseignement Supérieur de la Recherche et de l’Innovation”, the Region “Hauts-de-France”, and the ERDF Program of the European Union and “Métropole Européenne de Lille”. This project has received funding from the European Union’s Horizon 2020 Research and Innovation Programme under the Marie Skłodowska-Curie grant, agreement No. 847568, and was supported by the French government through the Programme Investissement d’Avenir (I-SITE UL-NE/ANR-16-IDEX-0004 ULNE), managed by the Agence Nationale de la Recherche, by the Programme d’Investissement d’Avenir “Mustart ANR-20-PAMR-0005”, by Institut National de la Santé et de la Recherche Médicale, by Université de Lille, and by Institut Pasteur de Lille. The NMR facilities were funded by the Région Hauts-de-France, CNRS, Institut Pasteur de Lille, the Fonds Européens de Développement Régional (FEDER), the Ministère de l’Enseignement supérieur, de la Recherche et de l’Innovation (MESRI), and Université de Lille.

Institutional Review Board Statement: Not applicable.

Informed Consent Statement: Not applicable.

Data Availability Statement: Data is contained within the article and supplementary material.

Conflicts of Interest: The authors declare no conflict of interest.

References

1. Patridge, E.; Gareiss, P.; Kinch, M.S.; Hoyer, D. An Analysis of FDA-Approved Drugs: Natural Products and Their Derivatives. *Drug Discov. Today* **2016**, *21*, 204–207. [[CrossRef](#)] [[PubMed](#)]
2. Sülsen, V.P.; Martino, V.S. (Eds.) *Sesquiterpene Lactones*; Springer International Publishing: Cham, Switzerland, 2018. [[CrossRef](#)]
3. Materazzi, S.; Benemei, S.; Fusi, C.; Gualdani, R.; De Siena, G.; Vastani, N.; Andersson, D.A.; Trevisan, G.; Moncelli, M.R.; Wei, X.; et al. Parthenolide Inhibits Nociception and Neurogenic Vasodilatation in the Trigeminovascular System by Targeting the TRPA1 Channel. *Pain* **2013**, *154*, 2750–2758. [[CrossRef](#)] [[PubMed](#)]

4. An, T.; Yin, H.; Lu, Y.; Liu, F. The Emerging Potential of Parthenolide Nanoformulations in Tumor Therapy. *Drug Des. Dev. Ther.* **2022**, *16*, 1255–1272. [[CrossRef](#)] [[PubMed](#)]
5. Freund, R.R.A.; Gobrecht, P.; Fischer, D.; Arndt, H.-D. Advances in Chemistry and Bioactivity of Parthenolide. *Nat. Prod. Rep.* **2020**, *37*, 541–565. [[CrossRef](#)] [[PubMed](#)]
6. Juliana, C.; Fernandes-Alnemri, T.; Wu, J.; Datta, P.; Solorzano, L.; Yu, J.-W.; Meng, R.; Quong, A.A.; Latz, E.; Scott, C.P.; et al. Anti-Inflammatory Compounds Parthenolide and Bay 11-7082 Are Direct Inhibitors of the Inflammasome. *J. Biol. Chem.* **2010**, *285*, 9792–9802. [[CrossRef](#)] [[PubMed](#)]
7. Liu, L.; Feng, L.; Gao, J.; Hu, J.; Li, A.; Zhu, Y.; Zhang, C.; Qiu, B.; Shen, Z. Parthenolide Targets NLRP3 to Treat Inflammasome-Related Diseases. *Int. Immunopharmacol.* **2023**, *119*, 110229. [[CrossRef](#)]
8. Mayer, R.J.; Allihn, P.W.A.; Hampel, N.; Mayer, P.; Sieber, S.A.; Ofial, A.R. Electrophilic Reactivities of Cyclic Enones and α,β -Unsaturated Lactones. *Chem. Sci.* **2021**, *12*, 4850–4865. [[CrossRef](#)]
9. Kamran, S.; Sinniah, A.; Abdulghani, M.A.M.; Alshawsh, M.A. Therapeutic Potential of Certain Terpenoids as Anticancer Agents: A Scoping Review. *Cancers* **2022**, *14*, 1100. [[CrossRef](#)]
10. Moujir, L.; Callies, O.; Sousa, P.M.; Sharopov, F.; Seca, A.M. Applications of Sesquiterpene Lactones: A Review of Some Potential Success Cases. *Appl. Sci.* **2020**, *10*, 3001. [[CrossRef](#)]
11. Sztiller-Sikorska, M.; Czyz, M. Parthenolide as Cooperating Agent for Anti-Cancer Treatment of Various Malignancies. *Pharmaceuticals* **2020**, *13*, 194. [[CrossRef](#)]
12. Neelakantan, S.; Nasim, S.; Guzman, M.L.; Jordan, C.T.; Crooks, P.A. Aminoparthenolides as Novel Anti-Leukemic Agents: Discovery of the NF- κ B Inhibitor, DMAPT (LC-1). *Bioorganic Med. Chem. Lett.* **2009**, *19*, 4346–4349. [[CrossRef](#)] [[PubMed](#)]
13. Ren, Y.; Kinghorn, A.D. Development of Potential Antitumor Agents from the Scaffolds of Plant-Derived Terpenoid Lactones. *J. Med. Chem.* **2020**, *63*, 15410–15448. [[CrossRef](#)] [[PubMed](#)]
14. Li, X.; Payne, D.T.; Ampolu, B.; Bland, N.; Brown, J.T.; Dutton, M.J.; Fitton, C.A.; Gulliver, A.; Hale, L.; Hamza, D.; et al. Derivatisation of Parthenolide to Address Chemoresistant Chronic Lymphocytic Leukaemia. *Med. Chem. Commun.* **2019**, *10*, 1379–1390. [[CrossRef](#)] [[PubMed](#)]
15. Carlisi, D.; Buttitta, G.; Di Fiore, R.; Scerri, C.; Drago-Ferrante, R.; Vento, R.; Tesoriere, G. Parthenolide and DMAPT Exert Cytotoxic Effects on Breast Cancer Stem-like Cells by Inducing Oxidative Stress, Mitochondrial Dysfunction and Necrosis. *Cell Death Dis* **2016**, *7*, e2194. [[CrossRef](#)] [[PubMed](#)]
16. Penthala, N.R.; Bommagani, S.; Janganati, V.; MacNicol, K.B.; Cragle, C.E.; Madadi, N.R.; Hardy, L.L.; MacNicol, A.M.; Crooks, P.A. Heck Products of Parthenolide and Melampomagnolide-B as Anticancer Modulators That Modify Cell Cycle Progression. *Eur. J. Med. Chem.* **2014**, *85*, 517–525. [[CrossRef](#)] [[PubMed](#)]
17. Carlisi, D.; Lauricella, M.; D’Anneo, A.; De Blasio, A.; Celesia, A.; Pratelli, G.; Notaro, A.; Calvaruso, G.; Giuliano, M.; Emanuele, S. Parthenolide and Its Soluble Analogues: Multitasking Compounds with Antitumor Properties. *Biomedicines* **2022**, *10*, 514. [[CrossRef](#)] [[PubMed](#)]
18. Häkkinen, S.T.; Soković, M.; Nohynek, L.; Ćirić, A.; Ivanov, M.; Stojković, D.; Tsitko, I.; Matos, M.; Baixinho, J.P.; Ivasiv, V.; et al. Chicory Extracts and Sesquiterpene Lactones Show Potent Activity against Bacterial and Fungal Pathogens. *Pharmaceuticals* **2021**, *14*, 941. [[CrossRef](#)] [[PubMed](#)]
19. Moreno Cardenas, C.; Çiçek, S.S. Structure-Dependent Activity of Plant Natural Products against Methicillin-Resistant Staphylococcus Aureus. *Front. Microbiol.* **2023**, *14*, 1234115. [[CrossRef](#)]
20. Cantrell, C.; Franzblau, S.; Fischer, N. Antimycobacterial Plant Terpenoids. *Planta Med.* **2001**, *67*, 685–694. [[CrossRef](#)]
21. Guzman, J.D.; Gupta, A.; Bucar, F.; Gibbons, S.; Bhakta, S. Antimycobacterials from Natural Sources: Ancient Times, Antibiotic Era and Novel Scaffolds. *Front. Biosci.* **2012**, *17*, 1861. [[CrossRef](#)]
22. Fischer, N.H.; Lu, T.; Cantrell, C.L.; Castañeda-Acosta, J.; Quijano, L.; Franzblau, S.G. Antimycobacterial Evaluation of Germacranolides in Honour of Professor G.H. Neil Towers 75th Birthday. *Phytochemistry* **1998**, *49*, 559–564. [[CrossRef](#)] [[PubMed](#)]
23. Frazier, C.P.; Engelking, J.R.; Read De Alaniz, J. Copper-Catalyzed Aerobic Oxidation of Hydroxamic Acids Leads to a Mild and Versatile Acylnitroso Ene Reaction. *J. Am. Chem. Soc.* **2011**, *133*, 10430–10433. [[CrossRef](#)] [[PubMed](#)]
24. Leach, A.G.; Houk, K.N. The Mechanism and Regioselectivity of the Ene Reactions of Nitroso Compounds: A Theoretical Study of Reactivity, Regioselectivity, and Kinetic Isotope Effects Establishes a Stepwise Path Involving Polarized Diradical Intermediates. *Org. Biomol. Chem.* **2003**, *1*, 1389–1403. [[CrossRef](#)] [[PubMed](#)]
25. Adam, W.; Krebs, O. The Nitroso Ene Reaction: A Regioselective and Stereoselective Allylic Nitrogen Functionalization of Mechanistic Delight and Synthetic Potential. *Chem. Rev.* **2003**, *103*, 4131–4146. [[CrossRef](#)] [[PubMed](#)]
26. Beier, P.; Mindl, J.; Štěrba, V.; Hanusek, J. Kinetics and Mechanism of Base-Catalysed Degradations of Substituted Aryl-N-Hydroxycarbamates, Their N-Methyl and N-Phenyl Analogues. *Org. Biomol. Chem.* **2004**, *2*, 562–569. [[CrossRef](#)] [[PubMed](#)]
27. Quadrelli, P.; Romano, S.; Piccanello, A.; Caramella, P. The Remarkable Cis Effect in the Ene Reactions of Nitrosocarbonyl Intermediates. *J. Org. Chem.* **2009**, *74*, 2301–2310. [[CrossRef](#)] [[PubMed](#)]
28. Jäger, C.; Haase, M.; Koschorreck, K.; Urlacher, V.B.; Deska, J. Aerobic C-N Bond Formation through Enzymatic Nitroso-Ene-Type Reactions. *Angew. Chem. Int. Ed.* **2023**, *62*, e202213671. [[CrossRef](#)] [[PubMed](#)]
29. Zhang, J.; Torabi Kohlbouni, S.; Borhan, B. Cu-Catalyzed Oxidation of C2 and C3 Alkyl-Substituted Indole via Acyl Nitroso Reagents. *Org. Lett.* **2019**, *21*, 14–17. [[CrossRef](#)]

30. Donohoe, T.J.; Chughtai, M.J.; Klauber, D.J.; Griffin, D.; Campbell, A.D. *N*-Sulfonyloxy Carbamates as Reoxidants for the Tethered Aminohydroxylation Reaction. *J. Am. Chem. Soc.* **2006**, *128*, 2514–2515. [[CrossRef](#)]
31. Prasanthi, A.V.G.; Begum, S.; Srivastava, H.K.; Tiwari, S.K.; Singh, R. Iron-Catalyzed Arene C-H Amidation Using Functionalized Hydroxyl Amines at Room Temperature. *ACS Catal.* **2018**, *8*, 8369–8375. [[CrossRef](#)]
32. Harris, L.; Mee, S.P.H.; Furneaux, R.H.; Gainsford, G.J.; Luxenburger, A. Alkyl 4-Chlorobenzoyloxycarbamates as Highly Effective Nitrogen Source Reagents for the Base-Free, Intermolecular Aminohydroxylation Reaction. *J. Org. Chem.* **2011**, *76*, 358–372. [[CrossRef](#)] [[PubMed](#)]
33. Sheldrick, G.M. Crystal Structure Refinement with *SHELXL*. *Acta Crystallogr. Sect. C Struct. Chem.* **2015**, *71*, 3–8. [[CrossRef](#)] [[PubMed](#)]
34. Sheldrick, G.M. A Short History of *SHELX*. *Acta Crystallogr. Sect. A Found Crystallogr.* **2008**, *64*, 112–122. [[CrossRef](#)] [[PubMed](#)]
35. Dolomanov, O.V.; Bourhis, L.J.; Gildea, R.J.; Howard, J.A.K.; Puschmann, H. *OLEX2*: A Complete Structure Solution, Refinement and Analysis Program. *J. Appl. Crystallogr.* **2009**, *42*, 339–341. [[CrossRef](#)]

Disclaimer/Publisher's Note: The statements, opinions and data contained in all publications are solely those of the individual author(s) and contributor(s) and not of MDPI and/or the editor(s). MDPI and/or the editor(s) disclaim responsibility for any injury to people or property resulting from any ideas, methods, instructions or products referred to in the content.